An Analysis of H II Regions in Dwarf Irregular Galaxies

S. B. Holmes
Department of Physics and Astronomy
College of Charleston

December 5, 2001

Acknowledgements

This work could not have been completed without the assistance of my advisors, **Phil Massey** (Lowell Observatory), **Knut Olsen** (CTIO/NOAO), **Chris Smith** (CTIO/NOAO), and **Laura Penny** (College of Charleston). Additionally, I am indebted to **Robert J. Dukes** (College of Charleston) and **Deidre Hunter** (Lowell Observatory).

Shadrian Holmes
November 2001

Contents

List of Figures

List of Tables

Chapter 1

Introduction

1.1 H II Regions in Dwarf Irregular Galaxies

The analysis of H II regions (regions of ionized hydrogen gas) reveal specific characteristics indicative of galactic structure, the interstellar medium (ISM) intrinsic to the galaxy, and stellar formation and evolution. Massive young stars, notably of spectral types O and B[1], emit on the order of 10^{37} ergs sec^{-1} ultraviolet flux. Radiating at a temperature of approximately 12000 to 50000 K, these young stars ionize surrounding gas an dust, resulting in H II regions.

Dwarf irregular galaxies are particularly rich in these young, hot stars. As a result, these galaxies are known for their numerous H II regions. H II region research and analysis has dated back to Hubble in 1925. Initially, detecting regions was a particularly crude process and entailed the rough approximation of the bubble-like regions (Figure 1.1).

Typically, the specific regions within the galaxy are chosen relative to a certain discernible limit of surface brightness. This limit corresponds to a level of 2×10^{-17} ergs sec^{-1} cm^{-2} arcsec^{-2}. Presently, there are individuals who seek to fine tune the "by-eye" approximation of the boundaries of the regions by generating computer programs. However, aside from the unproven use of computer algorithms, the measurement and detection precision of regions are highly dependent upon coverage and depth of the field.

The research presented in this paper is particularly unique, in that it utilizes deep, extremely wide-field images. As part of the *Local Group Survey*[2] project, the images have been taken on the 4-meter telescopes with Mosaic CCD cameras at Cerro Tololo Inter-American Observatory (CTIO) in Chile and Kitt Peak National Observatory (KPNO) in Arizona. These are presently the largest CCD imagers available on ground-based optical telescopes, having a field of view of one-half a degree on a side, or an area of 4.9×10^6 arsec^2.

[1] Stars are classified based on their temperature, or age. The classification scheme "O B A F G K M" is a sequence of temperature ranges, O being the hottest blue-white stars, M being the coolest, red stars.

[2] See section *Background*

Using these wide-field cameras to observe close (within 1.5 Mpc[3] dwarf irregular galaxies, provide the coverage and depth necessary to study documented regions and reveal undocumented ones. Extensive analysis of several of these close, dwarf irregular galaxies has been done in the past. However, research was limited to small telescopes with minimal field coverage (Figure 1.2)[4]. This paper closely examines the H II regions within WLM, NGC 6822, and Phoenix, comparing prior to present analysis.

[3] 1.5 Mpc is the maximum distance for Local Group membership, see section *Background*). 1 Mpc is 3.086×10^{18} cm

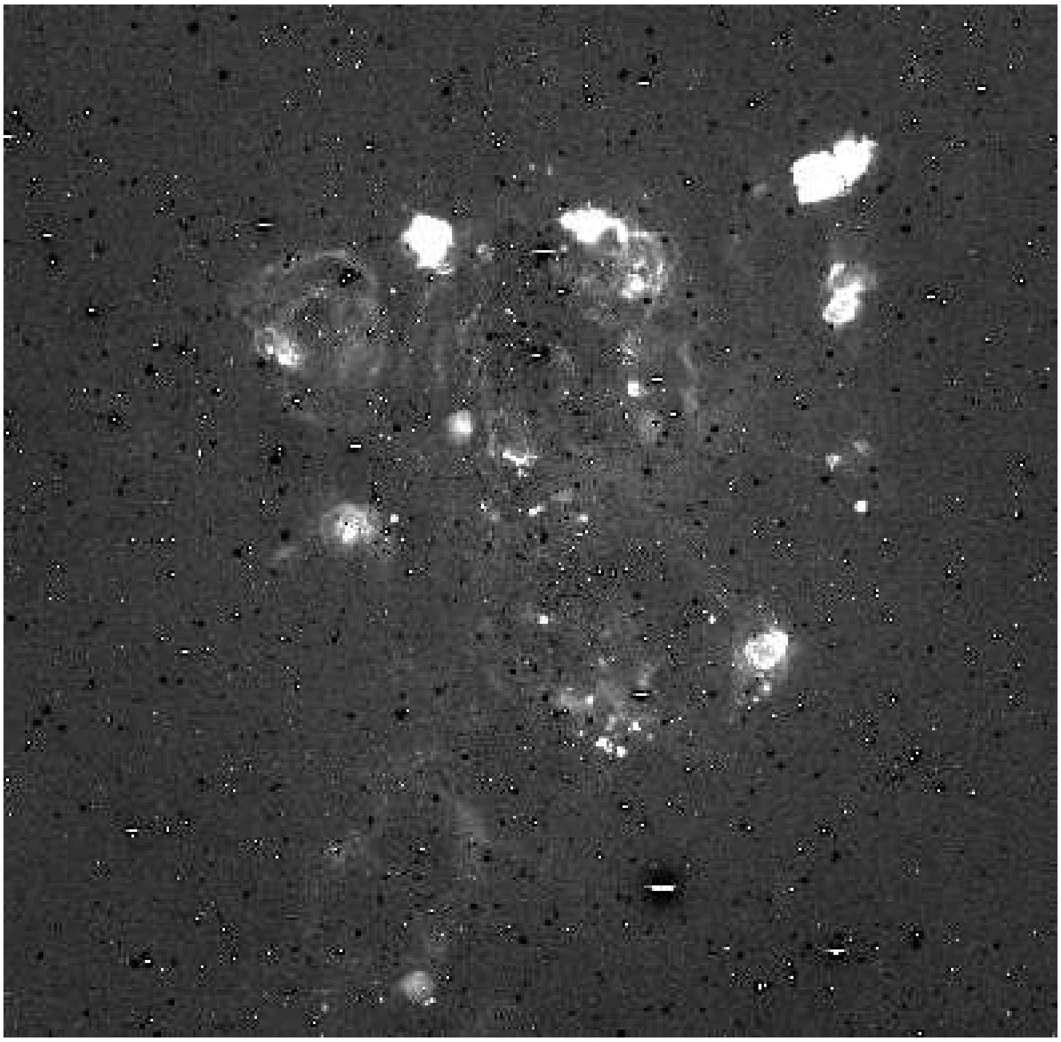

Figure 1.1: Image of H II regions within NGC 6822. The stars themselves have been subtracted. North is up

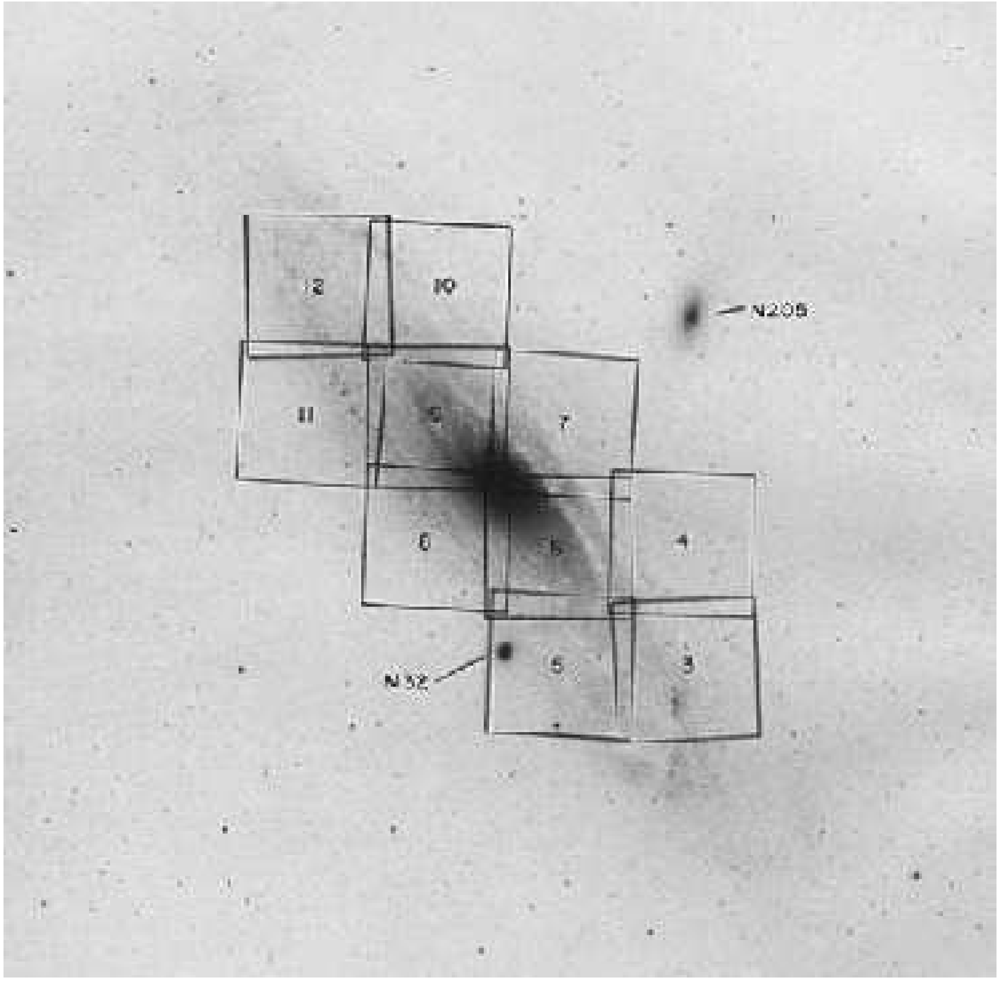

Figure 1.2: Selected regions of analysis in M31, prior to Mosaic use. Hodge, Paul. *Atlas of the Andromeda Galaxy.* University of Washington Press 1981.

Chapter 2

Background

2.1 The Local Group

First recognized by Edwin Hubble in 1936, the Local Group is but a coagulate system approximately 3 Mpc in diameter, the center of mass situated near M31 (Fig. 2.1). The galaxies are gravitationally bound; interacting with one another in a system of apparent poised fluidity. The proximity of the galaxies enable astronomers to study, in detail, stellar and galaxy evolution; supernovae, planetary nebulae, H II regions. The Local Group itself is composed of two massive spiral galaxies, the Milky Way and Andromeda (M31) galaxies, approximately three "medium sized galaxies" (M33, the Large Magellanic Cloud, the Small Magellanic Cloud, and over thirty-five other galaxies[1]). Hence, the Local Group is made up of varying galactic morphologies, or types.

Local Group membership has been debated since its 1936 incarnation. Van den Bergh [2] delineated several necessary characteristics for group membership. Perhaps most significant, a proposed galaxy should be located less than 1.5 Mpc from the Milky Way and should not be interacting with galaxies clearly beyond the Local Group.

2.2 Galactic Morphology

Galaxies are characterized by types, or morphologies (Fig. 2.2). Specifically, there are elliptical galaxies which branch off into normal spirals, like the Milky Way, and barred spirals. However, there is a grouping of galaxies known as irregular galaxies, which do not particularly obey the evolutionary "tuning fork" diagram. These galaxies show no particular structure and tend to vary in dimension.

[1] From "The Extended Local Group of Galaxies" http://www.astro.utu.fi/ rareko/AstroDic/LocalGroup.html

2.3 H II Regions

HII regions are regions of ionized hydrogen, as opposed to HI regions, which are neutral, molecular hydrogen regions. O and B stars initially form from a cloud of collapsing gas and dust (the components of ISM). A young protostar makes its first appearance as an "infrared source embedded inside"[3] this ISM cloud.

These young, hot stars excite H II regions. A typical O star radiates in an approximate temperature range of 20000 to 50000 K. Photons emitted from these stars that have energies greater than 13.6 eV, and a cooresponding UV flux of 10^{37} ergs $\sec^{-1}$, will ionize the molecular, ground-state hydrogen gas, H I, in the ISM surrounding the young star.

If the H II regions are in equilibrium, having constant volumes, then the rate in which photons are absorbed and ions are produced, must be equivalent to the rate that "free electrons and protons recombine to form neutral hydrogen atoms".[3] Recombining electrons will emit numerous photons of lower energy before entering the stable ground state of $n = 1$. Many of these discharged photons will fall in the range of visible wavelengths, 4000 Å to 7000 Å. The Balmer transition, $n = 3$ to $n = 2$, results in an emission of roughly 10^{39} erg $\sec^{-1}$ of Hα, having a visible wavelength of 6530 Å. Conveniently, H II regions may be detected by observing a field with an Hα filter, which is centered at 6563 Å.

The size of idealized models of H II regions, or Strömgren spheres, may be approximated as follows. If O and B stars emit an N number of photons per second, and assuming the region is in equilibrium, the number of hydrogen ions produced, n_H, equals the number of electrons freed, n_e, then r_s is the approximate Strömgren radius of the H II region, α is the tabulated recombination coefiicient describing the probability of an electron and proton forming a hydrogen atom,

$$r_s \approx (\frac{3N}{4\pi\alpha})^{1/3} n_H^{-2/3} \tag{2.1}$$

.

2.4 *The Local Group Survey* Project Data

The data used for this research has been aquired through the *Local Group Survey* project. The project is a "uniform survey of nearby galaxies selected on the basis of current star formation"[2]. Begun in 1999,the team includes Phil Massey, Lowell Observatory, Paul Hodge, University of Washington, Shay Holmes, College of Charleston, George Jacoby, WIYN, Nichole King, STSI, Knut Olsen, CTIO/NOAO, Abhijit Saha, KPNO/NOAO, Chris Smith, CTIO/NOAO. The project samples ten galaxies, M31, M33, NGC 6822, IC 1613, IC 10, WLM, Pegasus, Phoenix, Sextans A, and Sextans B, using the large NOAO 4-meter telescopes in the Northern and Southern Hemispheres: Kitt Peak National Observatory and Cerro Tololo Inter-American Observatory, respectively. The survey

[2]See Massey, http://www.lowell.edu/users/massey/lgsurvey.html

excludes the Milky Way and Magellanic Clouds since there are several independant surveys currently examining these popular Local Group member galaxies.

The data obtained through the *Survey* project is taken using wide-field Mosaic cameras, which are able to sample millions of stars on a single frame. The galaxies are observed in broadband filters, U, 3400 to 4000 Å, B, 3600 to 5000 Å, V, 5000 to 6500 Å, R, 5600 to 8800 Å, I, 7200 to 8800 Å, and narrowband filters, Hα, 6500 to 6620 Å, [SII], 6680 to 6780 Å, and [OIII], 3700 to 3780 Å.

Observations for the Southern galaxies NGC 6822, WLM, and Phoenix imaged in the R band and Hα are used in this sample of H II regions in dwarf irregualr galaxies.

2.5 The Dwarfs: NGC 6822, WLM, Phoenix

Dwarf irregular galaxies are significant laboratories in which to study galactic evolution and star formation. They have low metalicities[4] which make them "ideal" for analyzing "early stages of nucleosynthesis in galaxies and constraining the primordial helium abundance in the early universe'.[10]. Dwarf irregulars are typically rich in the young O and B stars, making them excellent candidates for H II region analysis.

2.5.1 NGC 6822

Barnard's galaxy, NGC 6822, Caldwell 57, type Ir+, in Sagittarius, was discovered by Barnard in 1884. NGC 6822 has particularly rich star formations regions. The HII regions have been analyzed by numerous individuals, the most extensive survey being completed by Paul Hodge (1988)[4].NGC 6822, Barnard's Galaxy, is the brightest of the dwarf irregular galaxies known. There are roughly sixteen bright stellar associations and thirty clusters. Significant regions of H II have been detected previously, including significant research done by Hodge, et al.(1988, 1989). NGC 6822 resides at a distance of 0.616 Mpc.

2.5.2 WLM

WLM, The Wolf-Lundmark-Melotte, galaxy was discovered in 1909 by Max Wolf, is a faint member of the Local Group, possessing an absolute magnitude of -14.7 mag (apparent B magnitude of 11 mag.). At 1.29 Mpc away, WLM sits on the edge of the Local Group.

2.5.3 Phoenix

ESO 245-7, Phoenix, has a dG morphological type and a distance of 396 kpc. Few papers have been published on this galaxy. It is believed that Phoenix is in transition from a dwarf irregular (dIrr) to a dwarf spheriodal (dSph).[3] It is

[3] Gallart et al. 2001

apparent that Phoenix shows a recent surge of star formation in its center. H I has yet to be discovered.

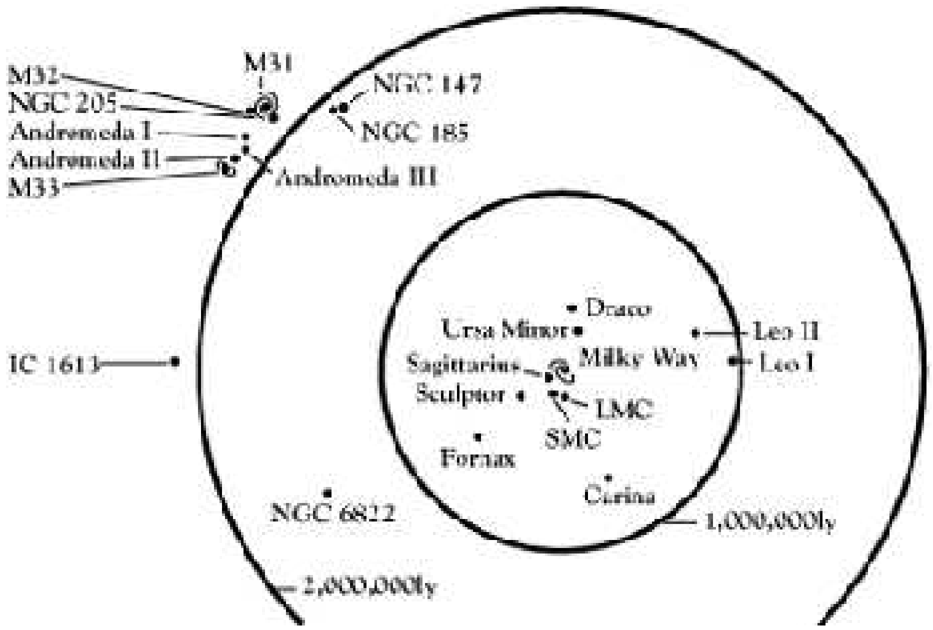

Figure 2.1: Relative circumference of the Local Group of galaxies. 1 pc = 3.26 ly.

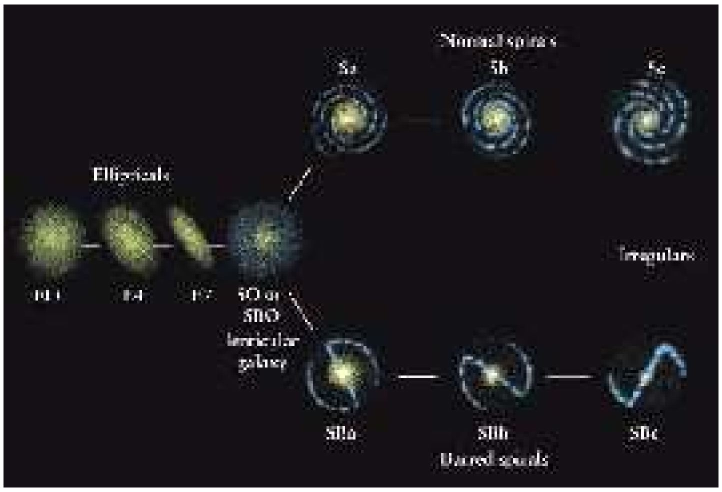

Figure 2.2: The “Tuning Fork” Diagram. Types of galaxies.

Chapter 3

Data

3.1 Observations and Reductions

There are observations of NGC 6822, WLM, and Phoenix for one night in August 2000 taken with the Blanco 4-meter using the Mosaic CCD at CTIO in the R and $H\alpha$ bands. The Mosaic CCD cameras are a composite of eight individual CCDs, with gaps in between. In order to produce a single gap-free image, a series of five to six dithered images are stacked, or combined using the IRAF task MSCred.[1] The whole process of image reduction is detailed in the SPLOG.[2]

Both the $H\alpha$ and the R images contain a mixture of stars and H II regions. In order to separate the stars, or the stellar continuum, from the gas of interest, a new image is created from the subtraction of the R from the Hα. The $H\alpha$ band, 6500 to 6620 Å, spans wavelengths included in the R band, 5600 to 8800 Å (Figure 3.1). To correctly subtract the images, the fluxes of several hundred stars were sampled in the R image and the corresponding $H\alpha$ image and were scaled to unity. The new H II region image can then be analyzed (Figure 3.2).

3.2 Calibration

In order to convert an image in units of pixels to units of standard flux, particularly ergs sec^{-1} cm^{-2}, a scale factor must be derived. Typically, along with the observations of the galaxies themselves, a standard star field is observed as well. This standard field contains stars of known fluxes and magnitudes and can be used for calibration purposes.

The scaling factor for the flux of the nebular line, in this case Hα, is calculated similar to the method implemented by Jacoby, et al. 1987,[8].

$$F_{NL} = \frac{(F_N)C_N 10^{0.4kA_N}}{T_L C 10^{0.4kA}}. \tag{3.1}$$

[1]Image Reduction and Analysis Facility, V2.11.3, MSCred, V.4.5 (May 4, 2001)
[2]See http://www.lowell.edu/users/massey/lgsurvey/splog2.html

Here, F_{NL} is the flux of the nebular line, F_N is the Hα flux measured relative a specific H II region, C_N is the number of counts per second for the corresponding region, k is the atmospheric extinction coefficient, A_N is the airmass of the image, T_L is the integral of the transmission curve for the Hα filter, and C and A are similar to C_N and A_N, but for standard star measurements.

3.3 Luminosity Functions

Luminosity functions are a measure of the number of H II regions in a galaxy brighter than a given luminosity as a function of luminosity, or

$$N(L) = AL^a dL. \tag{3.2}$$

Here N is the number of regions of luminosity L, A is a constant, and a is the slope of a linear fit to the bright side of the plot of $N(L)$ versus $\log L$.

Luminosity functions help to correlate the number of H II regions within a galaxy at specific luminosities to the stellar formation rates, i.e. the number of young O and B stars.

Measured fluxes are converted into luminosities by the relation

$$L = 4\pi D^2 (3 \times 10^{18} cm)^2 (\frac{1}{pc})^2 F, \tag{3.3}$$

where L is the luminosity, D is the diameter of the region in parsecs, and F is the measured flux in ergs sec^{-1} cm^{-2}.

Luminosity functions, because they reveal significant characteristics pertaining to the diversity of the H II regions within a galaxy, specifically, the number of O and B associations, can be used as a tool to examine star formation. From equation 3.2, the value for a is merely the slope of a linear fit to a histogram of the luminosity of the H II regions found. Therefore, it is useful to graphically depict the luminosity function. Values for a have been correlated for morphological types of galaxies. Kennicutt et al. (1988a) found, for irregular galaxies, a mean a-value of -1.7 [9]

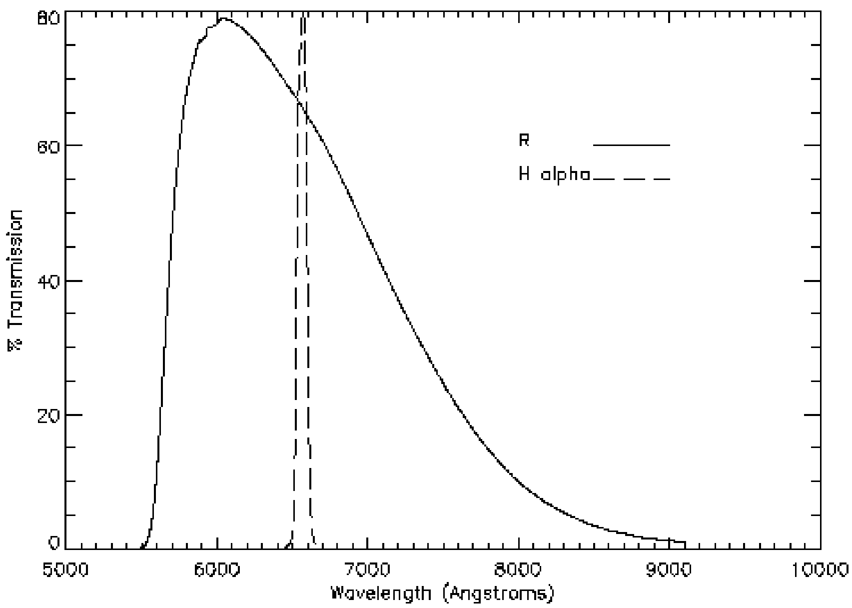

Figure 3.1: The percent transmission of the filter versus the wavelength

Chapter 4

Results

4.1 The Regions; Old and New

Regions were found implementing the techniques of Hodge, et al. (1988). The limiting discernible surface brightness for H II region detection is 2×10^{-17} ergs $\sec^{-1}$ cm^{-2} arc $\sec^{-2}$. The continuum subtracted images were displayed at this level and previously categorized H II regions were noted. New regions were then recorded. These new regions were defined according to apparent stellar associations. For NGC 6822, there are a total of 189 regions, 32 of them new. For WLM, there are a total of 45, with 35 new regions. For Phoenix, 6 total and 6 new regions were found.

4.2 The Regions of NGC 6822

Table 3.1 lists both the regions currently found as well as those found in the past. Additionally, the table displays the authors' designations used for the regions. Figures 4.1 through 4.14 display maps of the regions identified. Regions not drawn. Table 3.2 displays the coordinates, fluxes, and luminosities of the H II regions.

The luminosity function for NGC 6822, for the total number of 189 regions found, is shown in Figure 4.16. Here, the logarithm of the number of H II regions with a luminosity of $\log L$, is plotted versus the logarithm of the luminosities. According to the function

$$N(L) = AL^a dL, \tag{4.1}$$

the value of a can be determined by fitting a line to the bright side of the linearly binned histogram. The bright side corresponds to values greater than the specific turnoff function of the galaxy. Values greater than this L are fit well. Previous research, notably that done by Kennicutt et al. (1988*b*) and their predecessors, has determined that the H II region luminosity function can be approximated by the power-law function $N/(L) \propto \mathrm{L}^{-2\pm0.5}$. As delineated by Hodge et al.(1989), NGC 6822 has been shown to have a turnover at $L = 2 \times 10^{35}$

ergs $\sec^{-1}$. This "turnover" cooresponds to the degree at which incompleteness sets in and is approximately equivalent to the luminosity of a small H II region.

In Figure 4.16, the luminosity function of NGC 6822 is compared with the function found by Hodge et al. (1988). The slope of the linear fit to the bright side of the luminosity function ($L > 10^{35}$ ergs $\sec^{-1}$) is drawn on the graph and correlated to the 1988 slope value of $a = -1.6 \pm 0.1$ in order to correct for N II contamination. The value for $a = -1.8 \pm 0.1$. This differs from the 1988 value by approximately 10%; a difference that can be accounted for by the numerous, medium sized H II regions ($10^{35} < L < 10^{36}$ ergs $\sec^{-1}$) added to the previous total of 145 regions. The value of a agrees with the mean a values attributed to irregular galaxies, $a = -1.7$ (Kennicutt et al., 1988a).

Reference	Total Reported	No. New	Designation
Hubble (1925)	5	5	H + Roman numeral
Hodge (1969)	16	10	Ho + Arabic numeral
Kinman, Green, Mahaffey (1979)	3	3	K + Greek letter
Killen and Dufour (1982)	43	29	KD + Arabic numeral
Hodge, Kennicutt, Lee (1988)	145	110	HK + Arabic numeral
This paper (2001)	189	32	S + Arabic numeral
Total		189	

Table 4.1: The numbers of regions and their designations in NGC 6822

Region	RA	Dec	Log Hα Flux	Log Luminosity	Diameter	Diameter
S45	19:44:58	-14:43:02	1.55	33.18	68	203
S35	19:44:52	-14:44:53	1.76	33.39	90	268
HK108	19:45:19	-14:44:57	2.11	33.75	75	224
S52	19:45:12	-14:43:43	2.23	33.86	54	161
HK11	19:44:45	-14:45:47	2.27	33.90	77	231
HK82	19:45:04	-14:44:19	2.47	34.10	20	59
S67	19:44:43	-14:47:00	2.68	34.31	38	115
HK76	19:45:02	-14:43:23	2.84	34.48	109	327
S62	19:44:49	-14:49:03	2.86	35.00	56	167
S56	19:45:18	-14:44:21	2.92	34.55	67	201
HK3	19:44:33	-14:43:22	3.00	34.63	39	116
HK99	19:45:11	-14:48:14	3.08	34.71	12	35
S34	19:44:51	-14:44:41	3.10	34.73	40	120
S59	19:45:16	-14:49:14	3.10	34.73	46	137
S54	19:45:17	-14:43:58	3.15	34.78	79	235
HK101	19:45:12	-14:44:32	3.20	34.83	80	239
S68	19:44:42	-14:47:17	3.20	34.83	54	162
HK63	19:44:54	-14:48:15	3.24	34.87	54	161
S26	19:44:54	-14:44:07	3.24	35.00	51	153
S82	19:45:02	-14:58:20	3.26	34.90	47	139
HK35	19:44:49	-14:43:34	3.28	34.92	37	112
HK32	19:44:50	-14:43:43	3.29	34.92	46	138
KD21	19:44:54	-14:43:08	3.29	34.92	75	225
S69	19:44:39	-14:46:19	3.29	34.93	22	67
S20	19:44:52	-14:48:17	3.32	34.96	15	45
S46	19:44:56	-14:44:06	3.32	34.96	60	178
HK8	19:44:40	-14:52:01	3.33	34.97	50	149
HK94	19:45:09	-14:57:13	3.34	34.97	112	34
HK12	19:44:44	-14:46:24	3.36	34.99	81	241
S65	19:44:44	-14:47:03	3.36	34.99	61	182
HK80	19:45:04	-14:44:14	3.37	35.00	52	156
S44	19:44:56	-15:05:24	3.38	35.01	14	42
Hk86	19:45:07	-14:48:39	3.4	35.03	15	47

Table 4.2: NGC 6822 H II Region Details. The Hα flux is in units of 10^{-18} ergs $\sec^{-1}$ cm^{-2}. The Luminosity has units of 10^{-18} ergs $\sec^{-1}$. The diameters of the regions are in units of arcseconds and parsecs, respectively.

Region	RA	Dec	Log Hα Flux	Log Luminosity	Diameter	Diameter
HK51	19:44:51	-14:44:28	3.4	35.03	33	97
HK22	19:44:48	-14:45:33	3.41	35.05	60	178
HK93	19:45:09	-14:44:09	3.42	35.05	30	90
S51	19:45:09	-14:46:48	3.42	35.06	55	163
S4	19:44:39	-14:41:24	3.45	35.09	31	91
S19	19:45:00	-14:47:46	3.47	35.10	15	45
S81	19:45:01	-14:58:03	3.47	35.10	75	225
S24	19:44:48	-14:42:45	3.49	35.12	49	147
S64	19:44:44	-14:46:55	3.49	35.12	40	120
S78	19:45:02	-14:54:19	3.5	35.13	51	154
S13	19:45:00	-14:47:47	3.50	35.13	20	60
S85	19:44:18	-14:50:37	3.51	35.14	24	71
S63	19:44:44	-14:46:51	3.51	35.15	42	124
HK104+103	19:45:14	-14:46:42	3.53	35.16	33	99
S29	19:44:50	-14:43:22	3.55	35.18	9	26
HK17	19:44:47	-14:44:21	3.55	35.19	38	114
S2	19:44:35	-14:40:49	3.55	35.19	17	51
HK23	19:44:48	-14:46:50	3.56	35.19	98	292
S72	19:44:54	-14:45:36	3.57	35.20	37	110
HK27	19:44:49	-14:45:17	3.57	35.20	46	136
HK89	19:45:08	-14:57:40	3.57	35.20	11	34
S27	19:44:54	-14:43:54	3.57	35.20	45	136
HK15	19:44:47	-14:43:45	3.57	35.20	38	112
HK82	19:45:05	-14:44:15	3.58	35.21	20	59
S55	19:45:17	-14:44:33	3.58	35.21	29	85
HK5	19:44:39	-14:42:33	3.58	35.22	27	82
HK31	19:44:49	-14:45:50	3.59	35.22	31	91
HK105	19:45:16	-14:44:43	3.59	35.22	166	496
S74	19:45:08	-14:51:35	3.60	35.23	46	137
S61	19:45:01	-14:45:59	3.60	35.24	76	228
S17	19:45:00	-14:50:32	3.61	35.24	29	87
S18	19:44:59	-14:49:31	3.61	35.25	28	84
HK106	19:45:17	-14:45:11	3.63	35.26	52	154
HK88	19:45:08	-14:49:17	3.63	35.27	137	409
HK64(S25)	19:44:55	-14:43:59	3.63	35.27	55	163

Table 4.3: *continued* NGC 6822 H II Region Details. The Hα flux is in units of 10^{-18} ergs sec^{-1} cm^{-2}. The Luminosity has units of 10^{-18} ergs sec^{-1}. The diameters of the regions are in units of arcseconds and parsecs, respectively.

Region	RA	Dec	Log Hα Flux	Log Luminosity	Diameter	Diameter
S70	19:44:44	-14:44:57	3.64	35.27	100	299
HK48	19:44:51	-14:52:40	3.64	35.27	16	48
HK77	19:45:02	-14:43:43	3.66	35.29	43	130
S3	19:44:36	-14:41:06	3.66	35.29	56	167
HK85	19:45:07	-14:42:50	3.66	35.30	43	130
S15	19:44:53	-14:50:28	3.67	35.30	44	130
S21	19:44:50	-14:48:41	3.67	35.30	55	164
HK44	19:44:50	-14:44:16	3.67	35.31	44	131
S38	19:44:47	-14:43:33	3.69	35.32	36	106
S12	19:45:01	-14:47:26	3.69	35.33	44	131
S47	19:45:17	-14:45:06	3.69	35.33	33	99
HK28	19:44:48	-14:45:41	3.70	35.33	32	95
HK55	19:44:52	-14:44:10	3.70	35.33	46	137
S23	19:44:52	-14:42:16	3.71	35.34	15	45
HK20	19:44:47	-14:44:23	3.75	35.38	28	83
KD12	19:44:50	-14:43:15	3.75	35.39	66	197
S33	19:44:48	-14:43:54	3.76	35.39	49	146
K91	19:45:09	-14:56:49	3.79	35.42	15	44
S53	19:45:11	-14:43:54	3.79	35.42	58	174
S48	19:45:11	-14:45:09	3.79	35.42	66	198
HK21(S32)	19:44:47	-14:44:42	3.82	35.45	58	173
HK42	19:44:50	-14:43:42	3.82	35.45	50	150
S84	19:44:15	-14:46:34	3.82	35.45	40	119
S36	19:44:46	-14:44:09	3.85	35.49	42	124
S60	19:45:02	-14:46:05	3.86	35.49	24	72
S39	19:44:45	-14:43:41	3.87	35.50	55	165
HK68	19:45:05	-14:44:26	3.89	35.52	73	216
HK4	19:44:33	-14:43:44	3.90	35.54	51	152
HK70	19:45:00	-14:47:20	3.90	35.54	38	114
HK110	19:44:49	-14:43:23	3.9	35.54	40	119
S71	19:44:54	-14:46:17	3.91	35.55	43	128
S77	19:45:02	-14:54:09	3.91	35.55	53	158
HK109	19:44:48	-14:43:17	3.92	35.55	39	117
HK95	19:45:08	-14:57:30	3.92	35.56	17	50
S22	19:44:49	-14:42:58	3.92	35.56	12	36

Table 4.4: *continued* NGC 6822 H II Region Details. The Hα flux is in units of 10^{-18} ergs sec^{-1} cm^{-2}. The Luminosity has units of 10^{-18} ergs sec^{-1}. The diameters of the regions are in units of arcseconds and parsecs, respectively.

Region	RA	Dec	Log Hα Flux	Log Luminosity	Diameter	Diameter
HK41	19:44:49	-14:45:30	3.93	35.56	26	77
S8	19:44:51	-14:50:46	3.94	35.57	40	119
HK6	19:44:39	-14:51:32	3.94	35.57	27	82
S43	19:44:55	-14:42:10	3.94	35.57	53	160
HK37	19:44:49	-14:45:48	3.95	35.58	42	125
S10	19:45:00	-14:46:58	3.95	35.58	29	88
HK19	19:44:48	-14:43:22	3.95	35.58	40	120
S40	19:44:46	-14:43:21	3.97	35.60	60	181
S41	19:44:57	-14:42:06	3.97	35.61	21	63
HK72	19:44:60	-14:47:10	4.01	35.64	50	148
HK79	19:45:04	-14:44:01	4.01	35.64	58	172
HK38	19:44:50	-14:46:30	4.01	35.64	15	46
HK33	19:44:49	-14:43:53	4.02	35.65	54	162
HK73	19:45:0	-14:43:42	4.03	35.67	56	166
S73	19:44:59	-14:44:45	4.11	35.74	19	58
HK36	19:44:49	-14:44:30	4.12	35.76	38	115
HK78	19:45:04	-14:43:54	4.12	35.76	34	100
HK13	19:44:47	-14:43:56	4.13	35.76	33	100
S86	19:45:13	-14:57:41	4.16	35.79	50	150
S1	19:44:33	-14:42:23	4.16	35.79	17	49
HK66	19:44:57	-14:47:29	4.17	35.80	50	148
HK40	19:44:49	-14:44:26	4.17	35.81	38	114
HK102	19:45:13	-14:45:12	4.21	35.84	15	46
HK62	19:44:54	-14:43:36	4.24	35.87	37	110
S50	19:45:08	-14:45:24	4.24	35.88	123	368
HK107	19:45:18	-14:45:26	4.25	35.88	86	258
S14	19:45:00	-14:48:31	4.25	35.89	80	240
S30	19:44:50	-14:43:18	4.25	35.89	27	81
HK16	19:44:47	-14:44:01	4.26	35.89	37	110
S31	19:44:49	-14:43:21	4.27	35.90	20	59
HK59	19:44:54	-14:51:47	4.28	35.91	17	50
HK34	19:44:49	-14:45:32	4.28	35.92	30	88
HK65	19:44:56	-14:48:27	4.29	35.92	42	128
HK69	19:44:58	-14:47:47	4.29	35.92	32	97

Table 4.5: *continued* NGC 6822 H II Region Details. The Hα flux is in units of 10^{-18} ergs sec^{-1} cm^{-2}. The Luminosity has units of 10^{-18} ergs sec^{-1}. The diameters of the regions are in units of arcseconds and parsecs, respectively.

Region	RA	Dec	Log Hα Flux	Log Luminosity	Diameter	Diameter
HK7	19:44:39	-14:51:58	4.32	35.95	37	111
KD20	19:44:53	-14:48:38	4.33	35.96	57	171
S16	19:45:00	-14:50:09	4.33	35.97	18	53
S11	19:45:10	-14:54:31	4.37	36.00	15	43
KD8	19:44:38	-14:51:46	4.40	36.04	43	129
HK67	19:44:57	-14:47:39	4.41	36.04	32	96
S42	19:45:02	-14:41:37	4.43	36.06	18	54
HK81	19:45:04	-14:56:19	4.43	36.06	12	36
HK60	19:44:55	-14:42:42	4.46	36.09	17	52
HK87	19:45:08	-14:44:22	4.47	36.10	22	66
KD27	19:45:05	-14:57:35	4.47	36.10	37	111
HK87	19:45:08	-14:44:22	4.47	36.11	24	72
HK1	19:44:31	-14:47:17	4.54	36.17	87	258
KD9	19:44:48	-14:43:58	4.57	36.20	37	110
HK24	19:44:48	-14:52:41	4.60	36.23	32	95
KD33e	19:45:07	-14:47:31	4.66	36.29	15	46
S83	19:44:14	-14:44:46	4.67	36.30	31	92
S7	19:44:56	-14:50:31	4.77	36.40	45	134
HK83	19:45:05	-14:56:36	4.80	36.43	158	472
S6	19:44:43	-14:50:31	4.82	36.45	25	74
KD29	19:45:08	-14:48:36	4.82	36.45	42	125
KD24	19:44:58	-14:47:30	4.86	36.49	110	329
KD13e	19:44:49	-14:52:32	4.88	36.52	30	88
KD36e	19:45:17	-14:45:29	4.93	36.56	46	136
Ho6	19:44:49	-14:44:17	4.95	36.58	78	232
KD22e	19:44:53	-14:43:15	4.97	36.60	22	67
Ho1	19:44:33	-14:44:03	4.98	36.61	87	258
KD32e	19:45:05	-14:57:31	5.10	36.74	22	67
HK92	19:45:09	-14:44:35	5.11	36.74	148	441
HK2	19:44:32	-14:44:21	5.18	36.82	89	266
KD28e	19:44:57	-14:47:51	5.20	36.84	18	55
Ho12	19:44:57	-14:48:30	5.28	36.92	34	101
S76	19:45:12	-14:54:54	5.37	37.01	126	376
Kβ	19:44:33	-14:47:33	5.38	37.01	69	206
KD13	19:44:50	-14:52:58	5.5	37.14	41	124

Table 4.6: *continued* NGC 6822 H II Region Details. The Hα flux is in units of 10^{-18} ergs sec^{-1} cm^{-2}. The Luminosity has units of 10^{-18} ergs sec^{-1}. The diameters of the regions are in units of arcseconds and parsecs, respectively.

Region	RA	Dec	Log Hα Flux	Log Luminosity	Diameter	Diameter
Ho5	19:44:38	-14:51:08	5.51	37.14	182	544
Ho7	19:44:49	-14:46:13	5.51	37.14	98	293
Ho10	19:44:52	-14:51:59	5.54	37.17	48	144
KD1e	19:44:31	-14:41:36	5.56	37.19	27	82
S49	19:45:10	-14:45:26	5.64	37.28	168	501
Kα	19:44:31	-14:48:24	5.65	37.28	55	164
S9	19:45:02	-14:46:55	5.66	37.29	14	422
HII	19:44:32	-14:44:44	5.67	37.30	152	454
HK26	19:44:49	-14:52:28	5.83	37.46	46	136
Ho16	19:45:16	-14:45:36	5.84	37.48	155	463
HIII	19:44:34	-14:42:18	5.96	37.59	239	714
Ho15	19:45:11	-14:48:46	6.31	37.94	265	792
HI	19:44:32	-14:42:04	6.65	38.28	196	584
HV	19:44:52	-14:43:07	7.10	38.74	170	508
HX	19:45:05	-14:43:24	7.12	38.75	254	759

Table 4.7: *continued* NGC 6822 H II Region Details. The Hα flux is in units of 10^{-18} ergs sec^{-1} cm^{-2}. The Luminosity has units of 10^{-18} ergs sec^{-1}. The diameters of the regions are in units of arcseconds and parsecs, respectively.

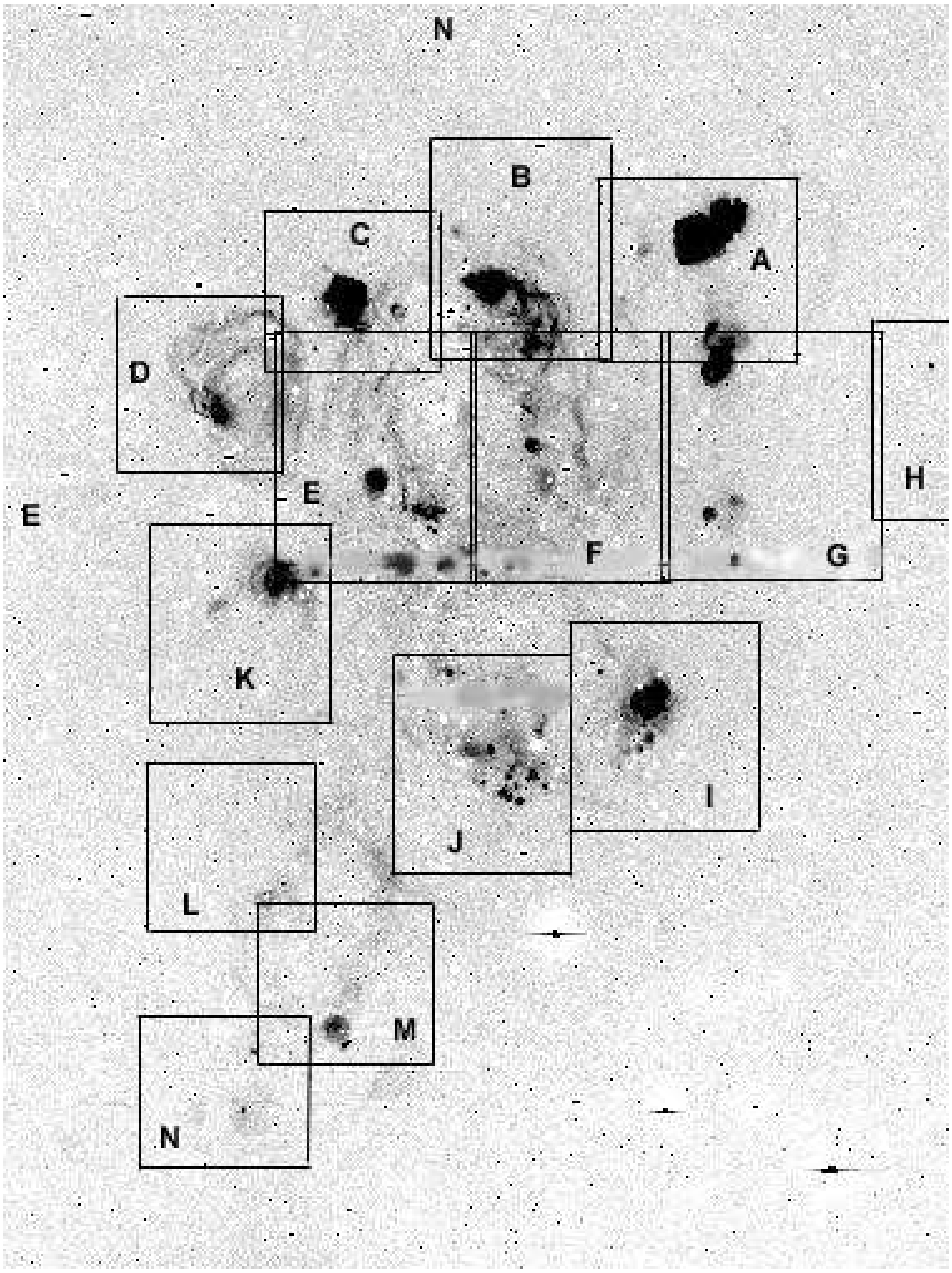

Figure 4.1: NGC 6822, Continuum Subtracted Hα image. The overlayed regions correspond to the detailed close-ups in the following pages.

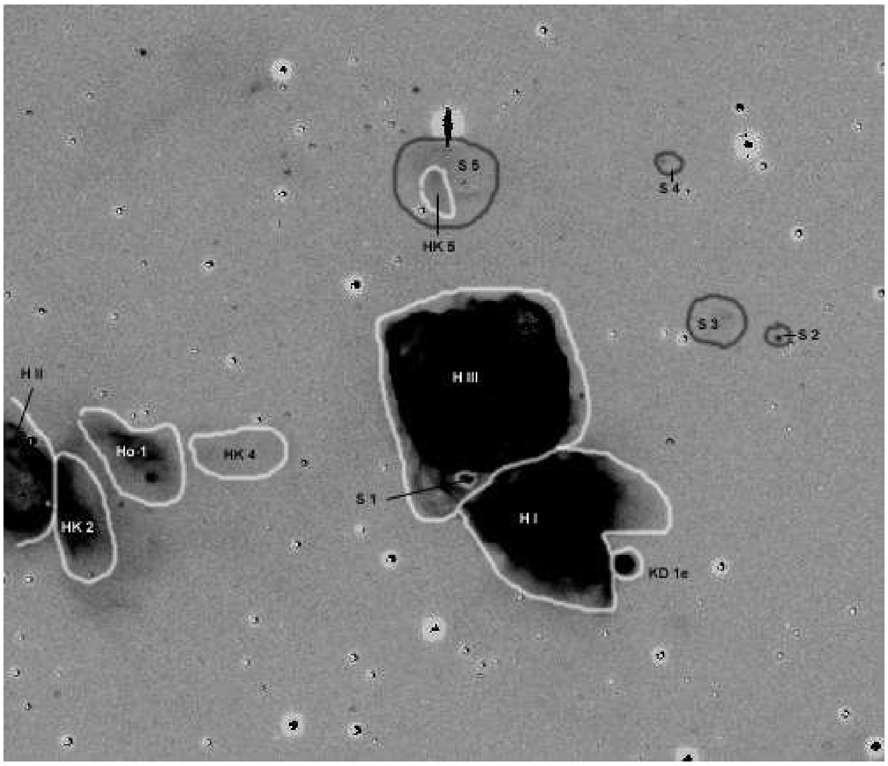

Figure 4.2: Region A, continuum subtracted frame

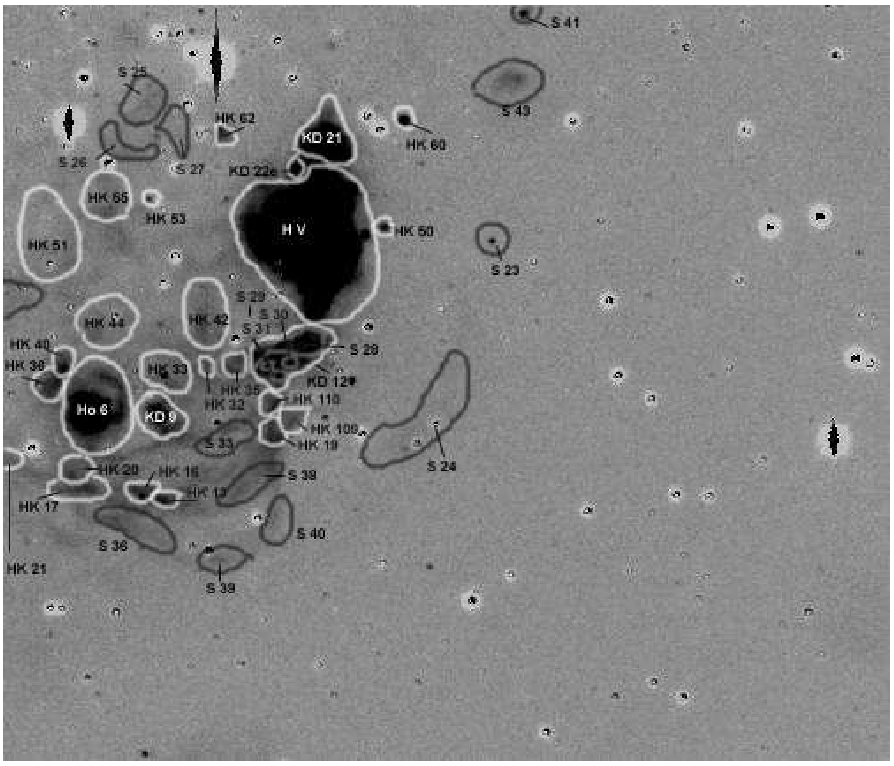

Figure 4.3: Region B, continuum subtracted frame

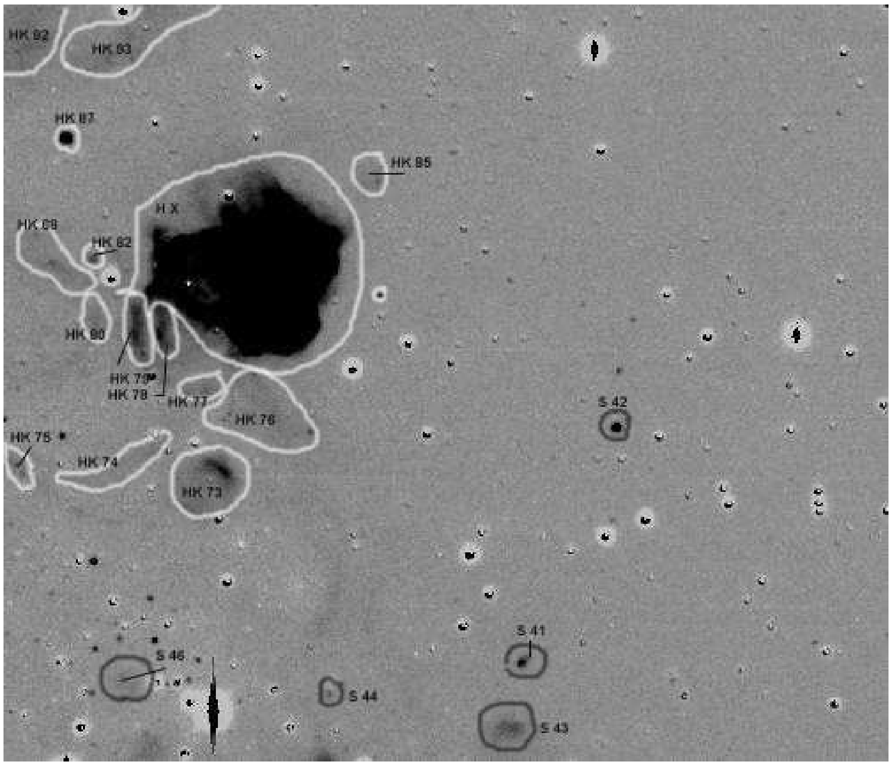

Figure 4.4: Region C, continuum subtracted frame

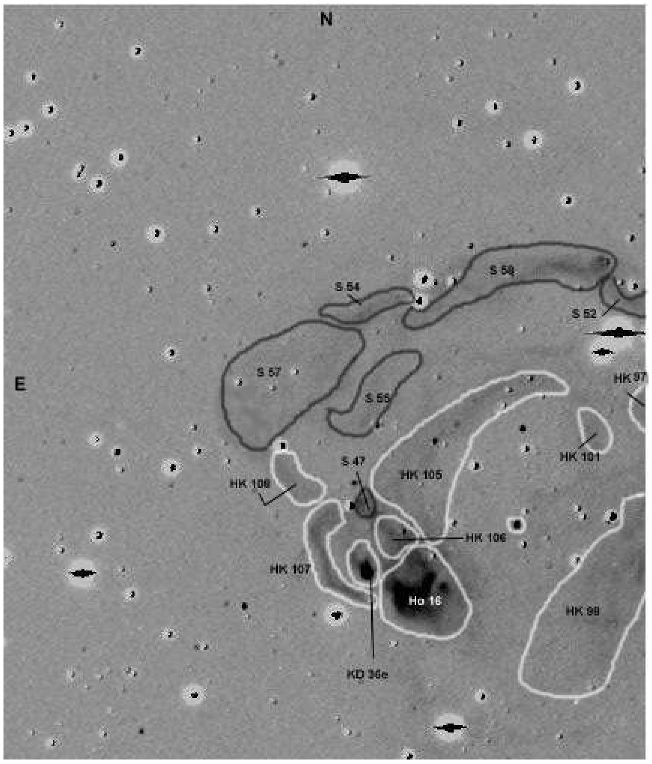

Figure 4.5: Region D, continuum subtracted frame

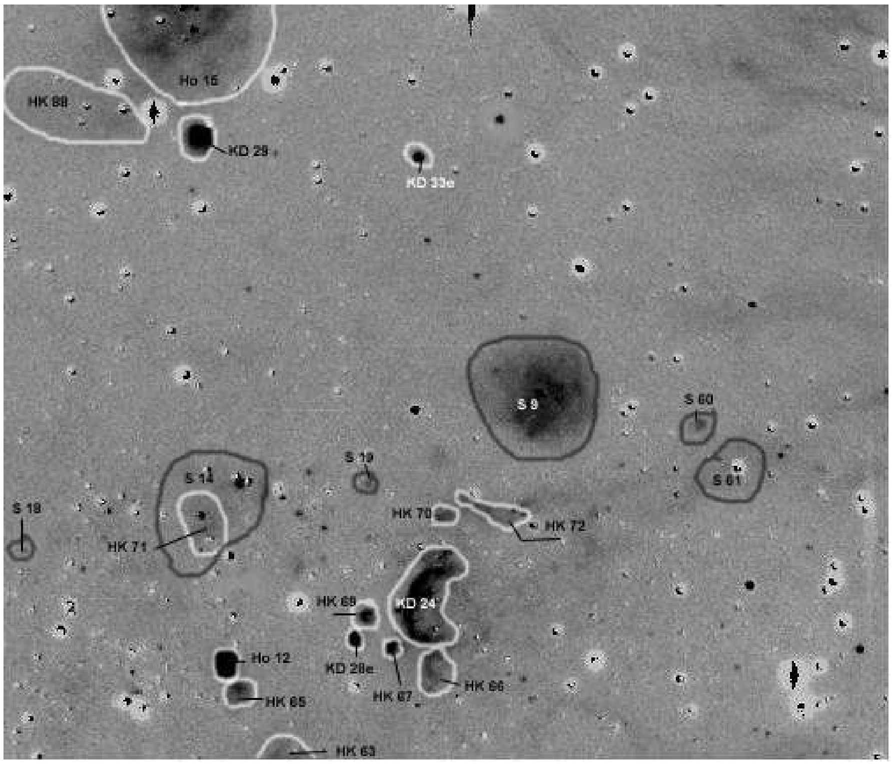

Figure 4.6: Region E, continuum subtracted frame

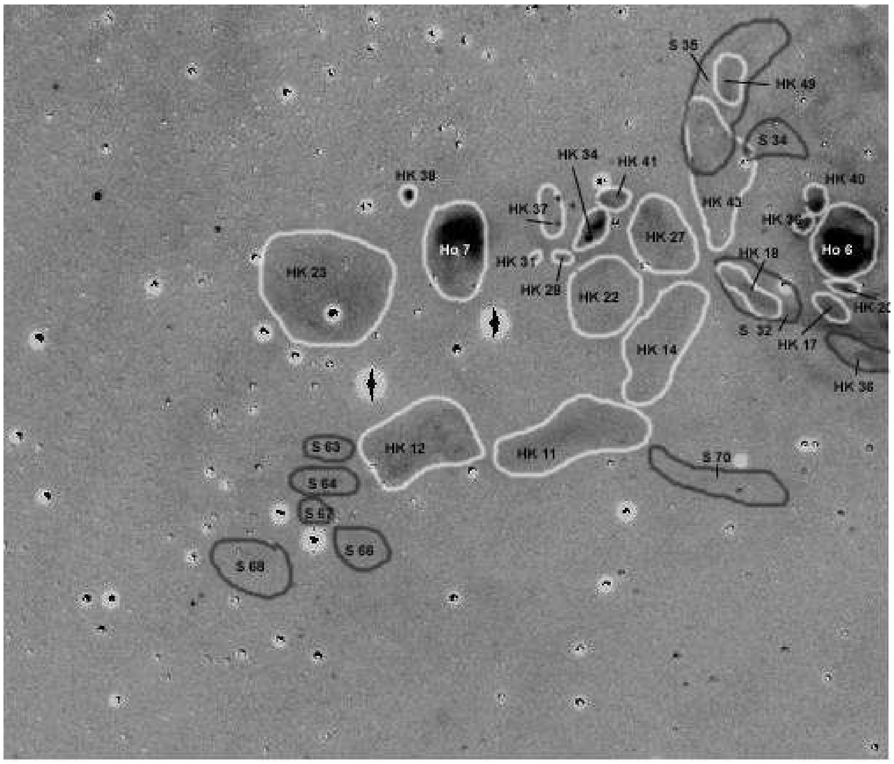

Figure 4.7: Region F, continuum subtracted frame

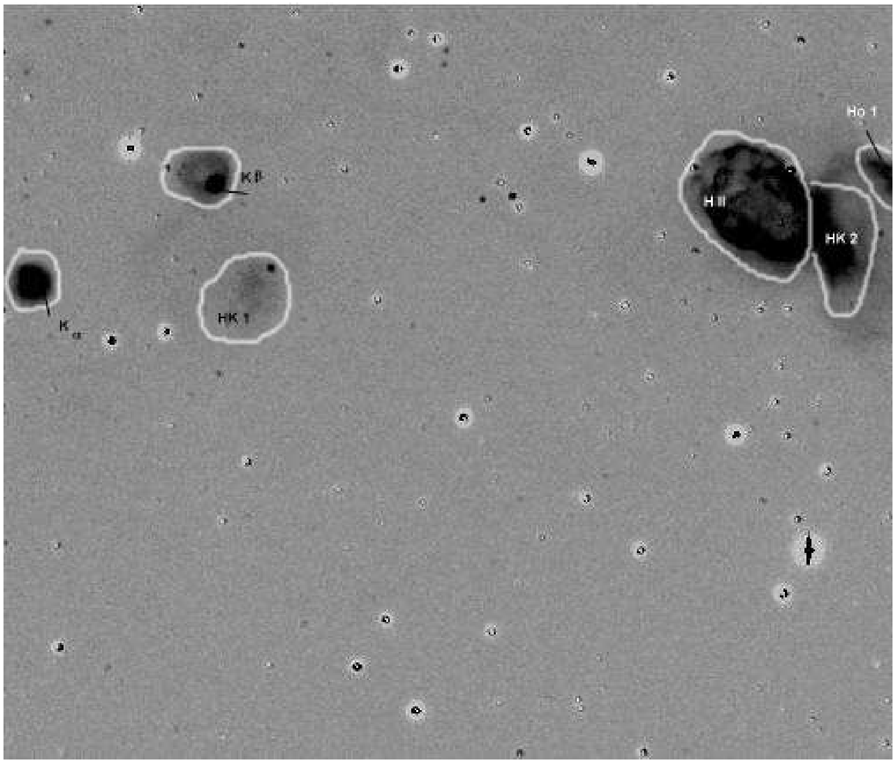

Figure 4.8: Region G, continuum subtracted frame

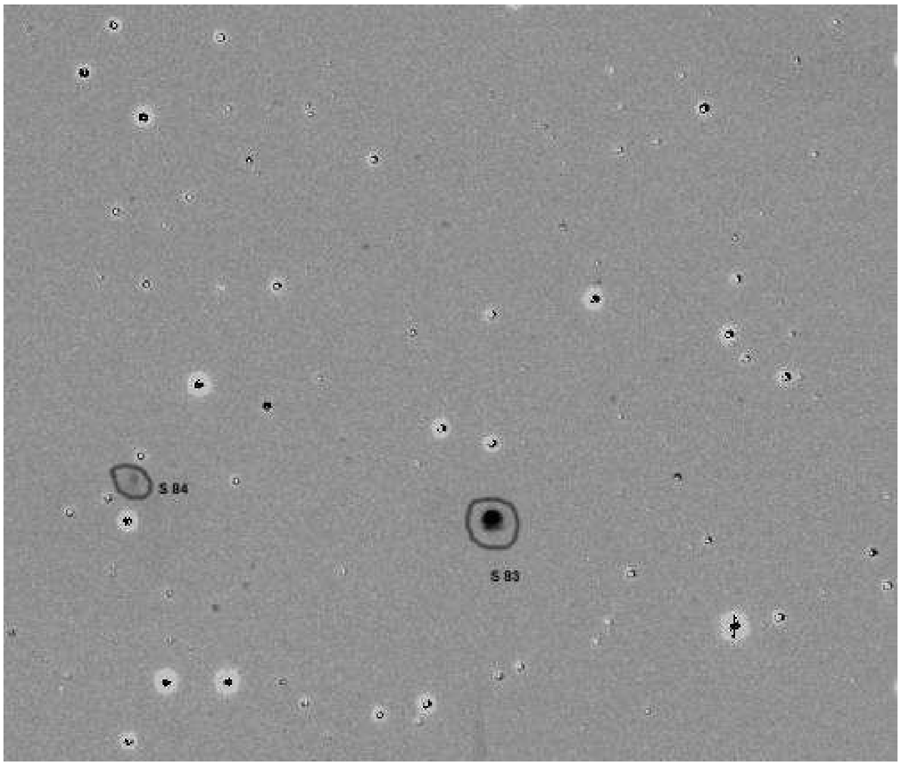

Figure 4.9: Region H, continuum subtracted frame

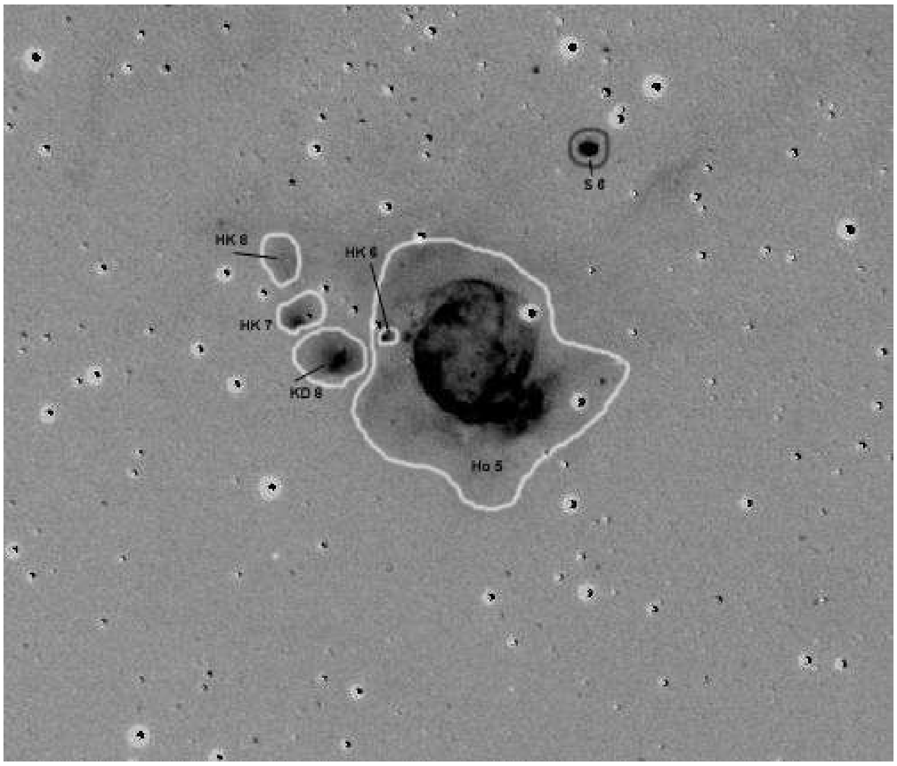

Figure 4.10: Region I, continuum subtracted frame

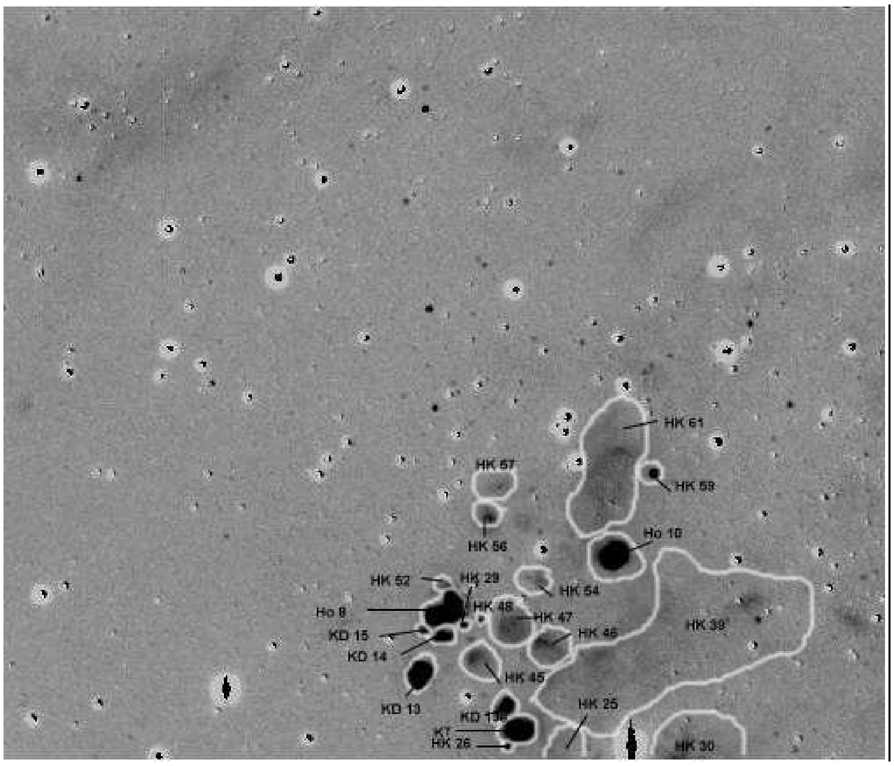

Figure 4.11: Region J, continuum subtracted frame

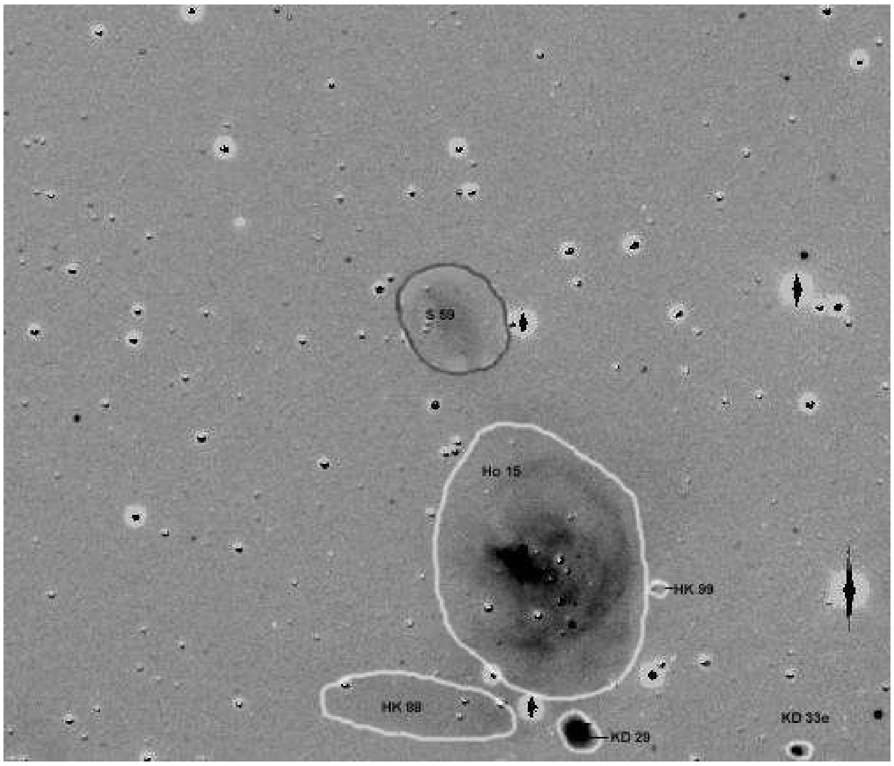

Figure 4.12: Region K, continuum subtracted frame

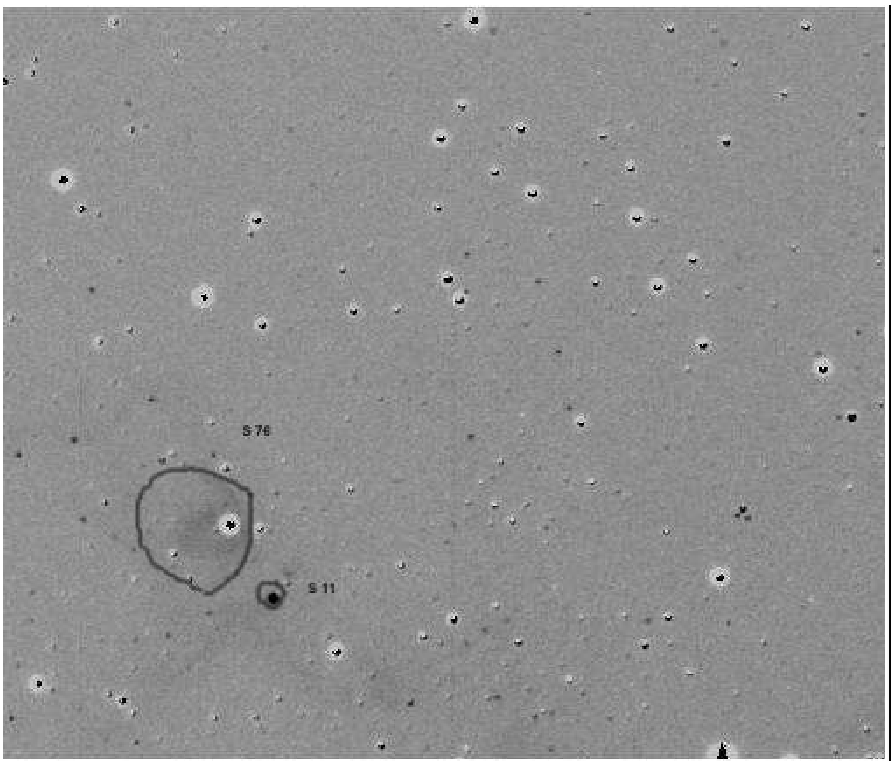

Figure 4.13: Region L, continuum subtracted frame

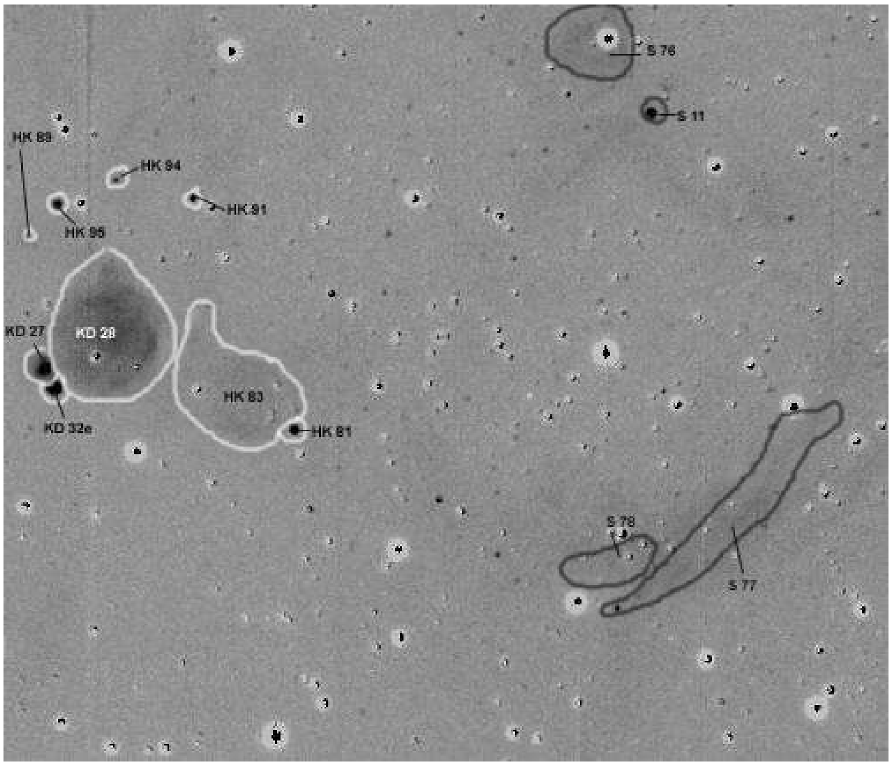

Figure 4.14: Region M, continuum subtracted frame

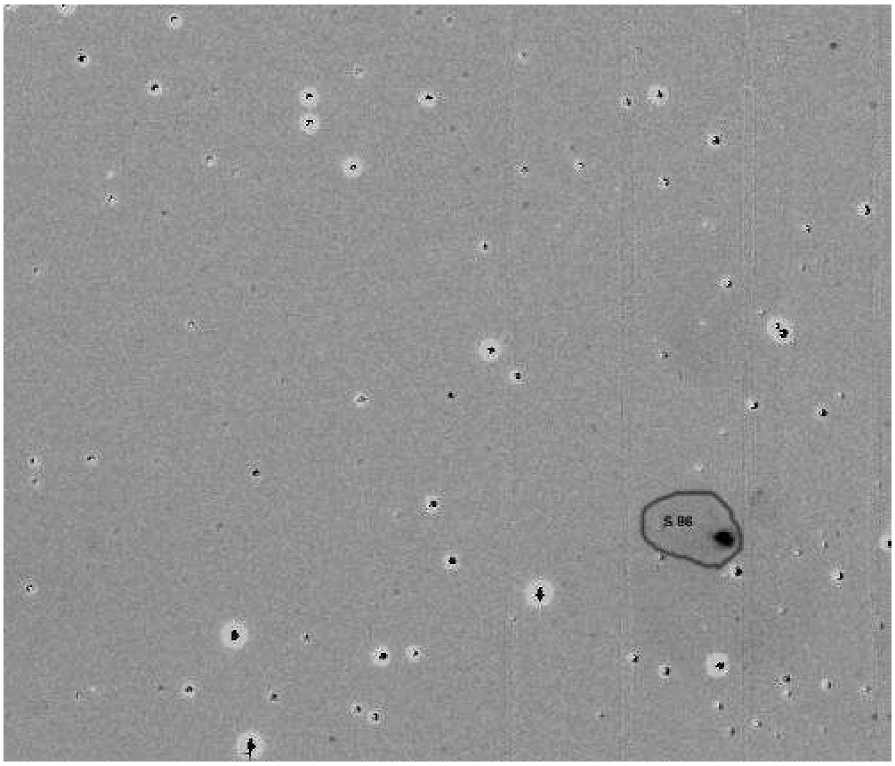

Figure 4.15: Region N, continuum subtracted frame

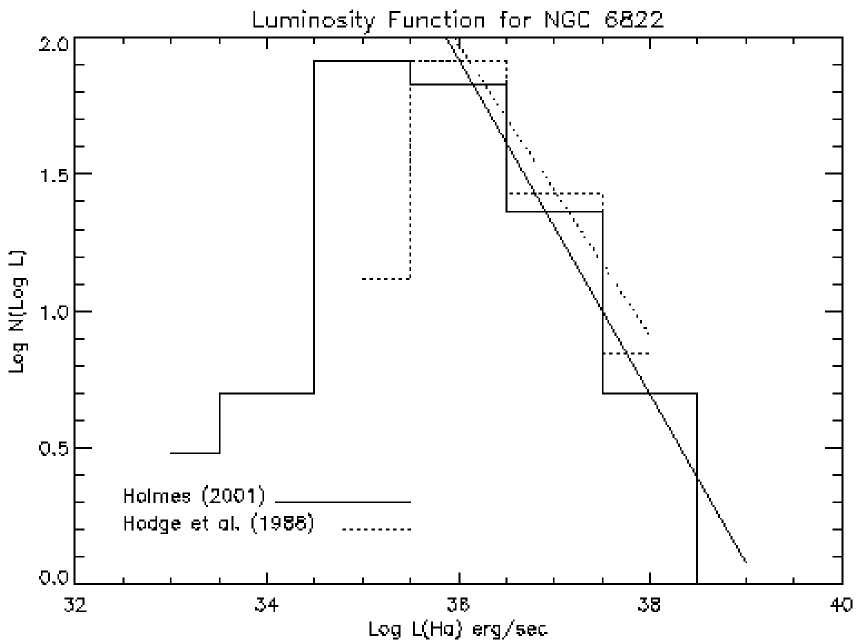

Figure 4.16: The Luminosity Function for NGC 6822. Here, the function found in this paper is compared with that obtained by Hodge et al. (1988).

4.3 The Regions of WLM

A similar procedure to that used for NGC 6822 was implemented with the WLM dwarf. While Hodge and Miller (1995) did not find a value of incompleteness for the luminosity function, there appears to be one here for $L > 10^{35}$ (Figure 19). Only when incorporating this limiting turnover value could the data be fit well by a slope a corresponding to -1.5 ± 0.1. Comparing this to the 1995 value of $a = -1.2 \pm 0.1$, there is a 25% difference, which again can be contributed to the numerous small to medium sized regions found in this paper.

Reference	Total Reported	No. New	Designation
Hodge and Miller (1995)	21	21	HM + Arabic numeral
This paper (2001)	45	35	S + Arabic numeral

Table 4.8: Designations for H II Regions in WLM

Region	RA	Dec	Log Hα Flux[1]	Log Luminosity[2]	Diameter[3]	Diameter[4]
S21	00:01:55	-15:26:28	2.01	34.00	42	190
S17	00:01:53	-15:27:38	2.42	34.41	52	233
S22	00:01:47	-15:27:16	2.83	34.82	59	263
S6	00:01:57	-15:28:29	2.93	34.91	27	120
S31	00:01:56	-15:24:08	3.02	35.00	32	1423
HM4	00:01:57	-15:26:36	3.05	35.04	14	61
S30	00:01:55	-15:27:60	3.10	35.09	51	231
S19	00:01:59	-15:25:55	3.19	35.18	29	130
S24	00:01:57	-15:30:14	3.25	35.23	55	244
S23	00:01:54	-15:30:05	3.28	35.27	57	256
S20	00:01:59	-15:25:31	3.30	35.28	32	143
S11	00:02:01	-15:27:51	3.30	35.29	32	144
HM9	00:01:60	-15:26:54	3.32	35.30	85	382
S9	00:02:00	-15:28:32	3.33	35.32	32	142
HM7	00:01:58	-15:29:03	3.35	35.33	57	257
S29	00:01:56	-15:29:15	3.40	35.38	44	199
S3	00:01:54	-15:28:34	3.41	35.40	35	156
S25	00:01:50	-15:29:29	3.51	35.50	72	323
S26	00:01:49	-15:29:41	3.51	35.50	76	342
S14	00:01:57	-15:27:03	3.54	35.53	15	68
S10	00:02:01	-15:28:47	3.55	35.53	94	420
S16	00:01:52	-15:27:06	3.60	35.58	56	249
HM1	00:01:54	-15:27:33	3.79	35.78	25	114
S7	00:01:57	-15:28:26	3.79	35.78	54	242
HM8	00:01:57	-15:26:60	3.83	35.81	23	102
S27	00:01:47	-15:28:01	3.86	35.84	104	464
S1	00:01:60	-15:27:29	3.90	35.90	18	81
S5	00:01:55	-15:28:30	3.98	35.97	44	197
S13	00:01:60	-15:29:51	4.02	36.00	74	333
HM12	00:01:57	-15:29:26	4.09	36.08	23	103
S8	00:01:57	-15:29:13	4.11	36.09	48	213
S12	00:02:01	-15:29:36	4.17	36.15	45	203
S18	00:01:56	-15:25:60	4.19	36.18	114	513
HM15	00:01:56	-15:26:53	4.25	36.23	77	347
S28	00:01:55	-15:29:08	4.26	36.25	99	442
HM14	00:01:57	-15:26:48	4.27	36.26	28	125
S15	00:01:54	-15:26:52	4.34	36.32	53	239
S4	00:01:56	-15:28:37	4.46	36.45	92	411
S2	00:01:59	-15:27:24	4.56	36.55	20	89
HM2	00:01:55	-15:26:54	4.56	36.55	63	280
HM9	00:02:01	-15:28:04	4.61	36.59	47	213
HM21	00:02:02	-15:27:41	4.62	36.60	45	201
HM16	00:01:60	-15:27:27	4.67	36.65	32	141
HM10	00:01:56	-15:29:19	5.43	37.41	40	177

[1] units of 10^{-18} ergs sec^{-1} cm^{-2}
[2] units of 10^{-18} ergs sec^{-1}
[3] units of arcseconds
[4] units of parsecs

Table 4.9: Particulars of H II Regions in WLM

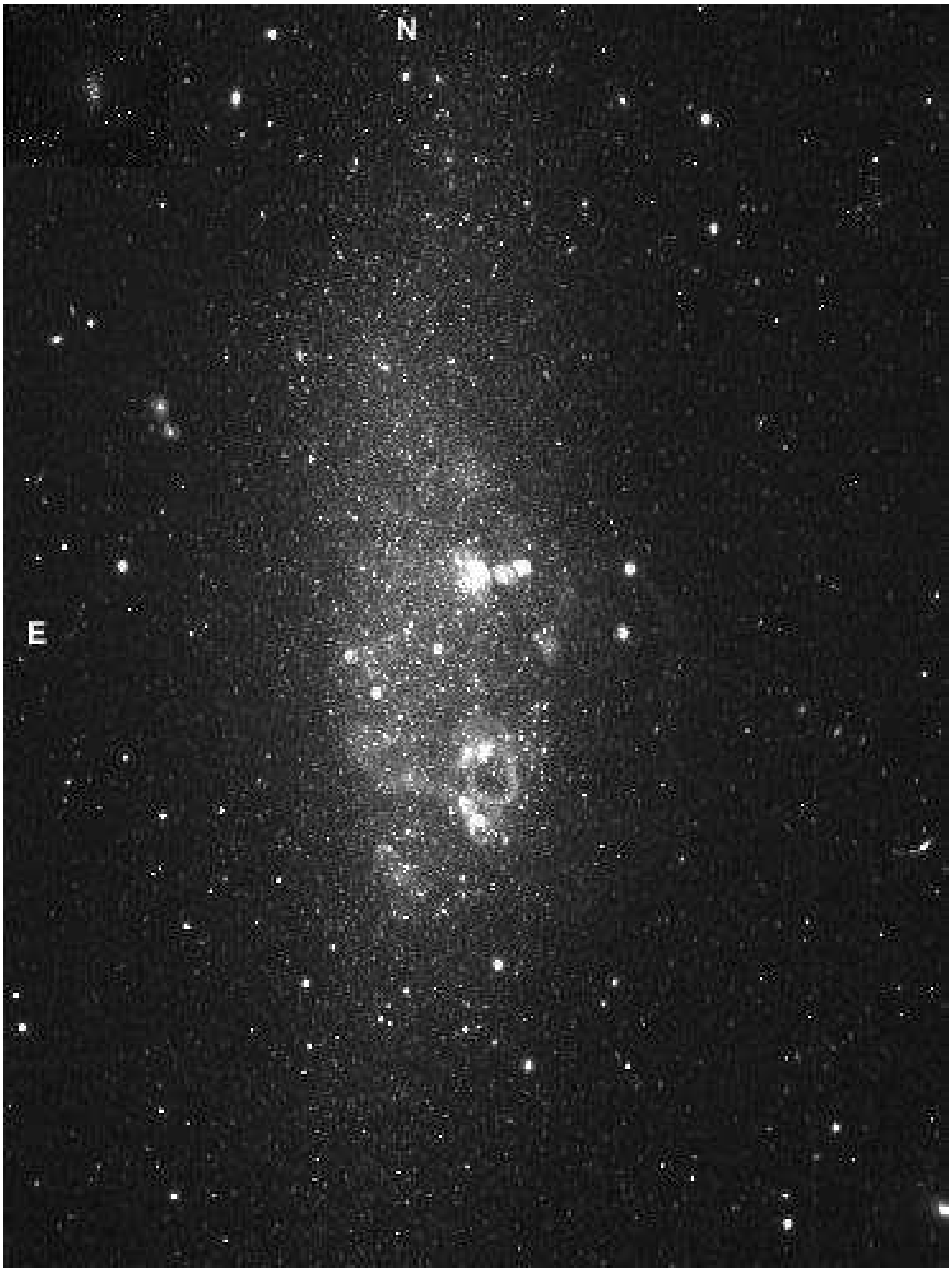

Figure 4.17: WLM in the Hα filter.

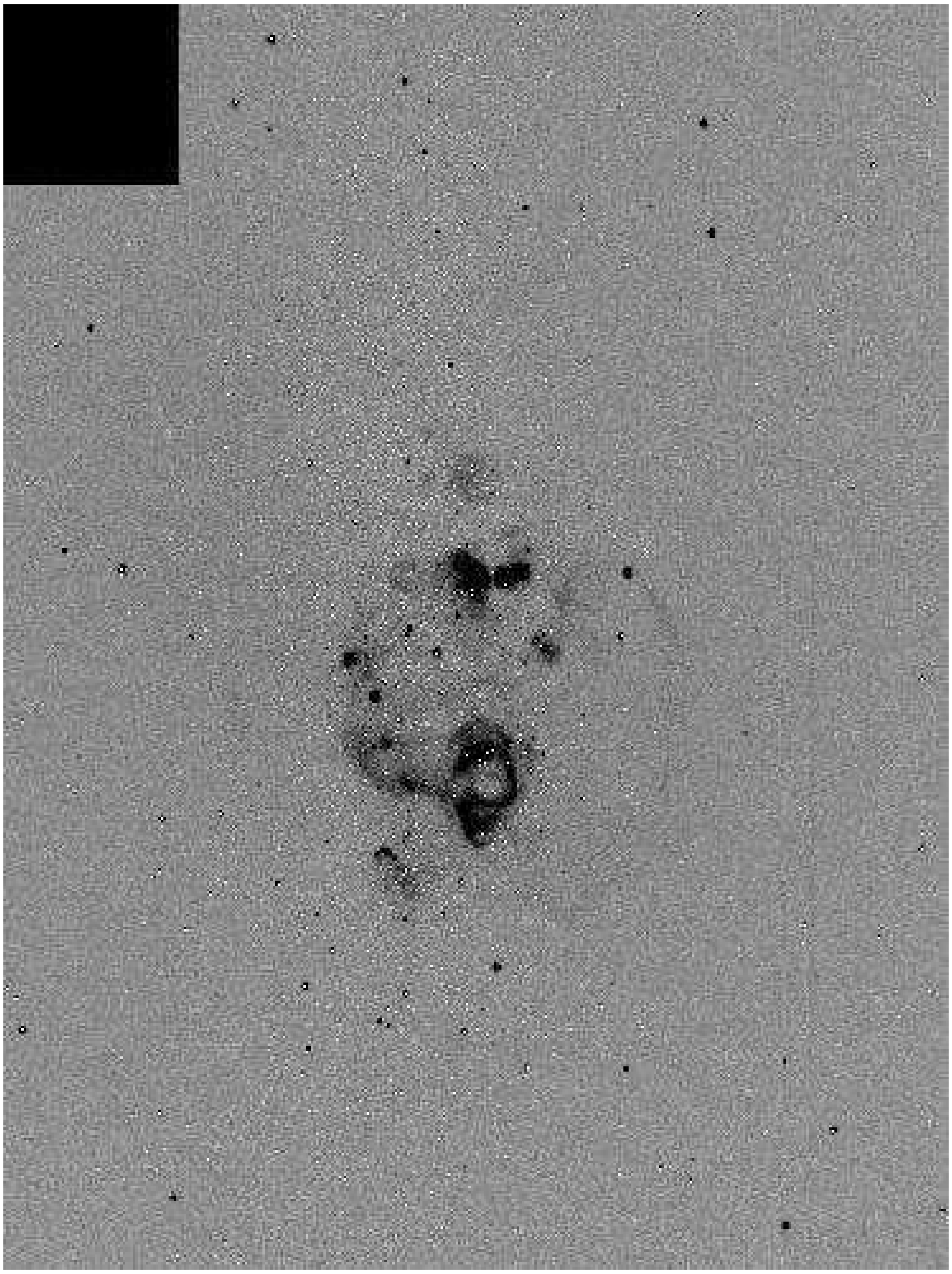

Figure 4.18: Continuum Subtracted WLM

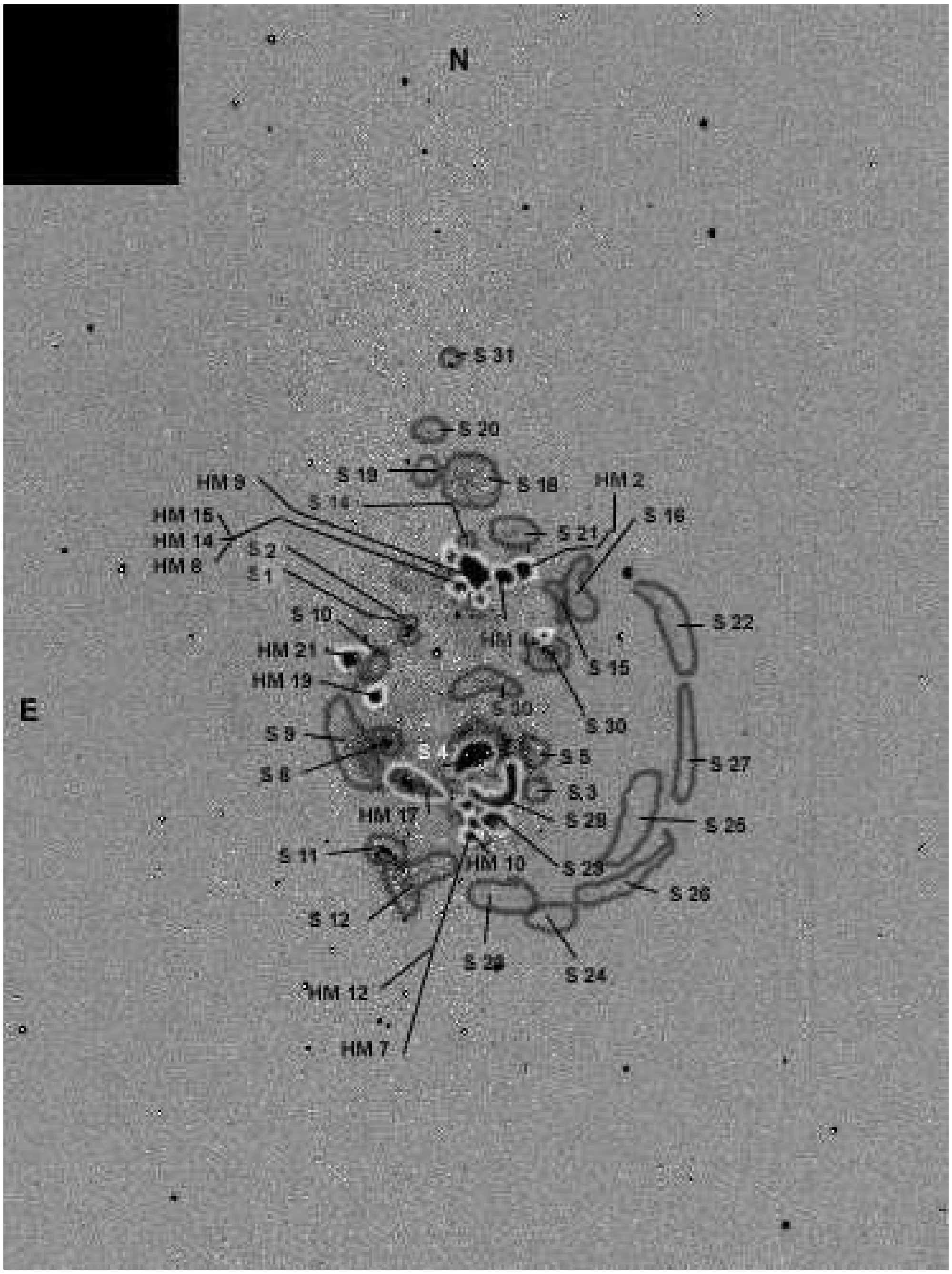

Figure 4.19: The H II Regions of WLM

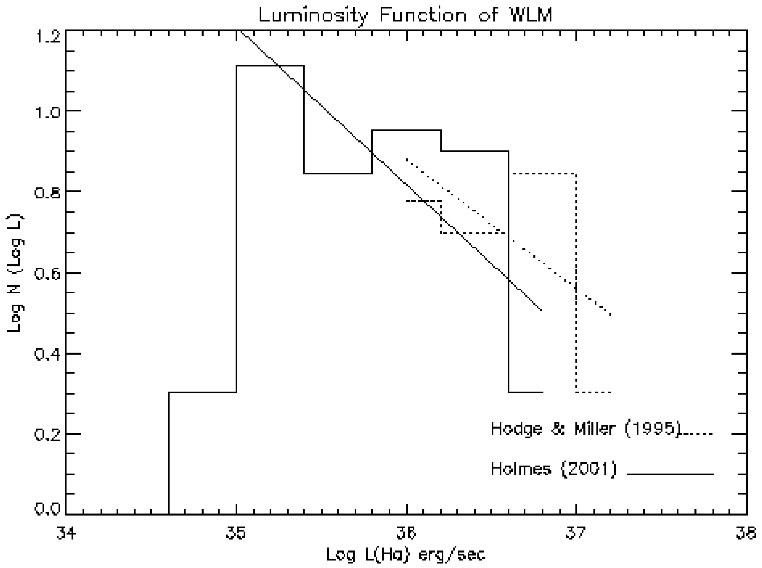

Figure 4.20: The Luminosity Function of WLM. The function obtained in this paper is compared to the function Hodge and Miller (1995) obtained.

4.4 The Regions of Phoenix

The H II regions found for the Phoenix dwarf are the first designated. Respectively, they are labeled *A* through *F*. The luminosity function, though rather sparse, still can be approximated by the slope $a = -1.7 \pm 0.1$ if correlated to the Hodge and Miller (1995) data, plotted with bins of 0.25. This a-value still correlates with the values of a for other irregular galaxies.

Region	RA	Dec	Log Hα Flux[5]	Log Luminosity[6]	Diameter[7]	Diameter[8]
C	01:51:04	-44:27:12	2.85	34.10	13	24
D	01:51:07	-44:26:49	3.68	34.93	7	13
G	01:50:59	-44:27:03	3.70	34.94	8	15
B	01:51:05	-44:26:42	3.84	35.08	13	25
E	01:51:02	-44:26:03	3.99	35.24	29	55
F	01:50:59	-44:26:57	4.05	35.29	7	14
A	01:51:06	-44:26:56	4.50	35.74	8	16

[5] units of10^{-18} ergs sec^{-1} cm^{-2}
[6] units of 10^{-18} ergs sec^{-1}
[7] units of arcseconds
[8] units of parsecs

Table 4.10: H II Regions in Phoenix

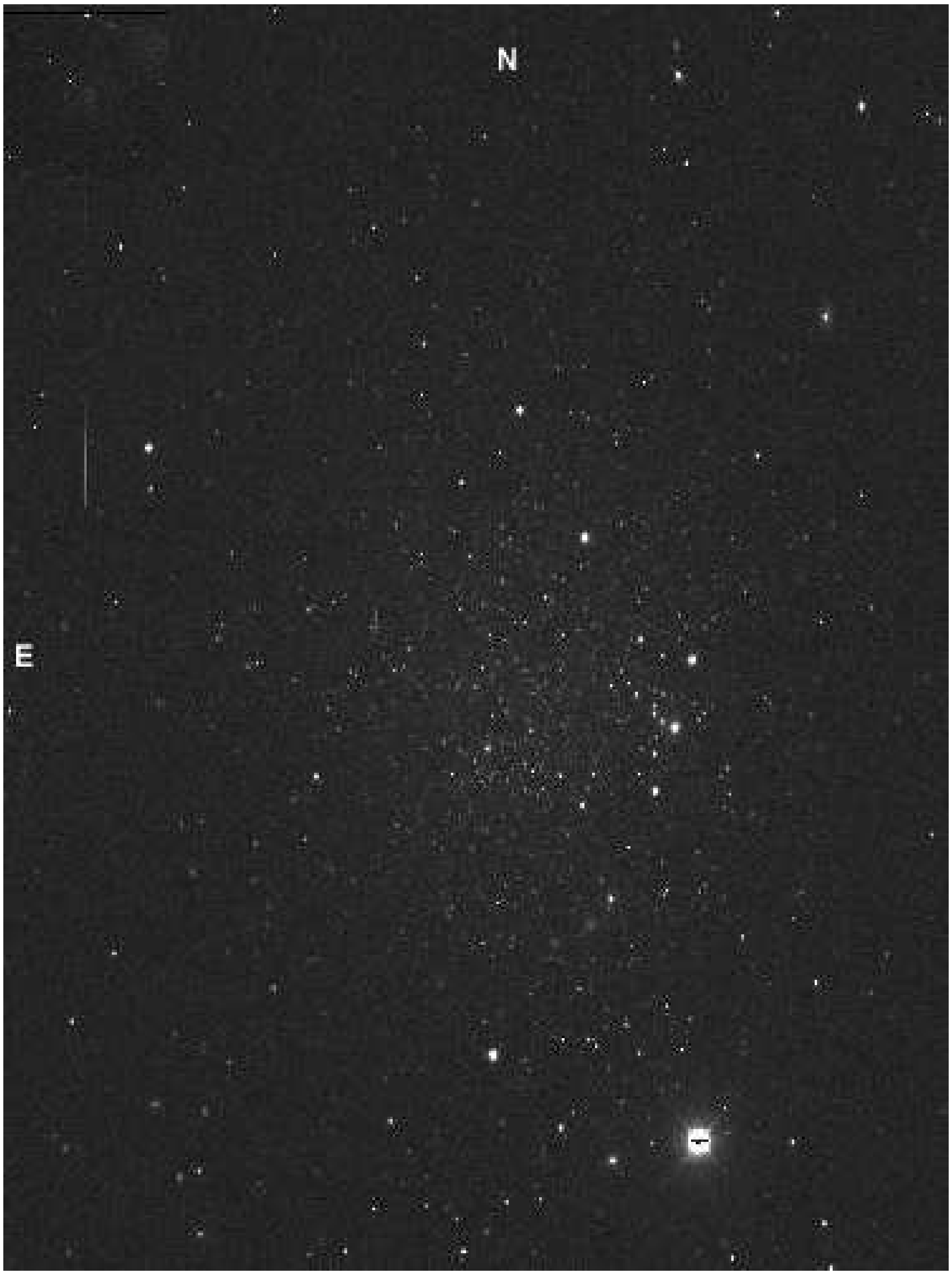

Figure 4.21: Phoenix observed with the Hα filter.

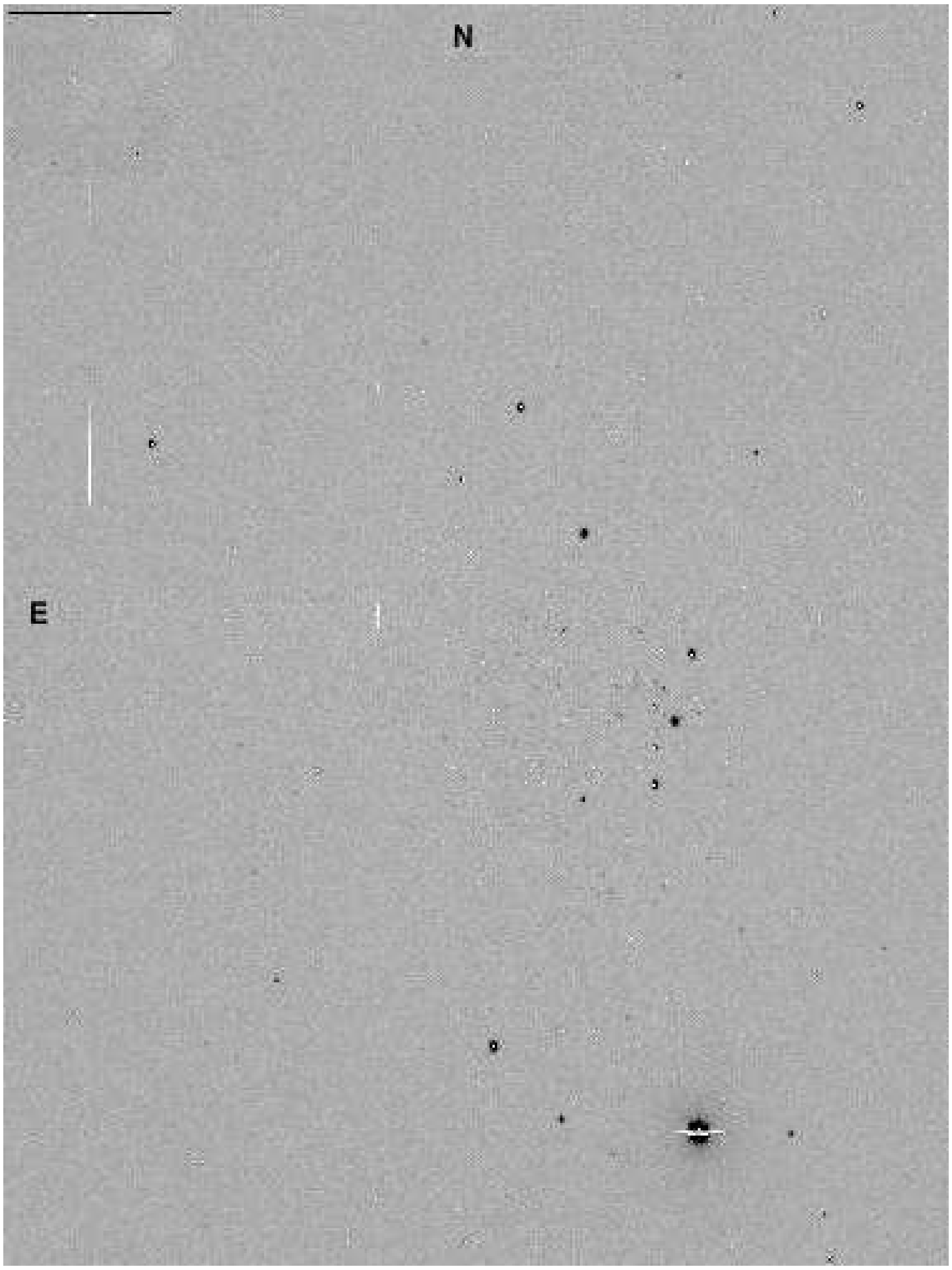

Figure 4.22: Continuum Subtracted Phoenix

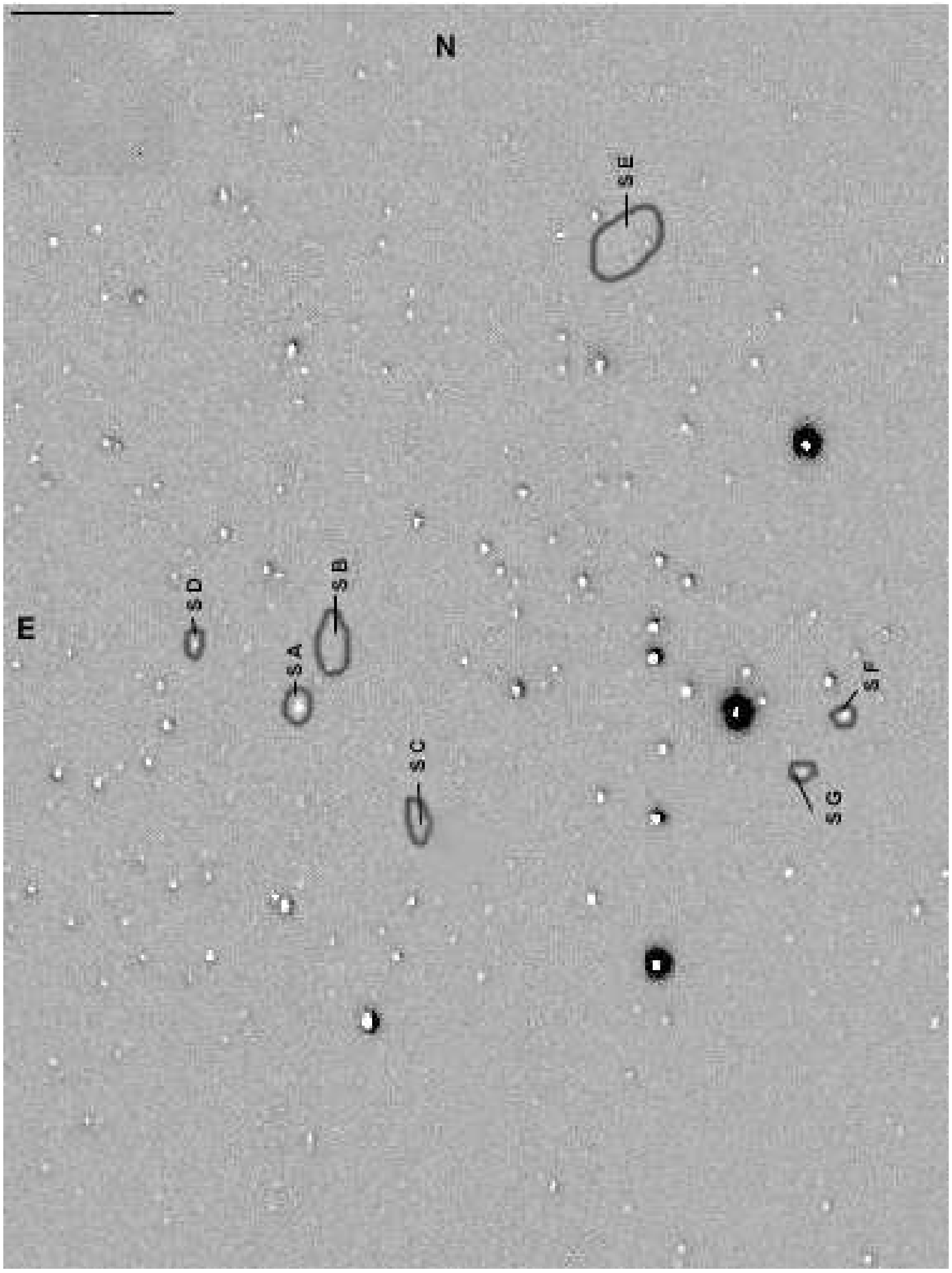

Figure 4.23: The H II Regions of Phoenix (zoomed)

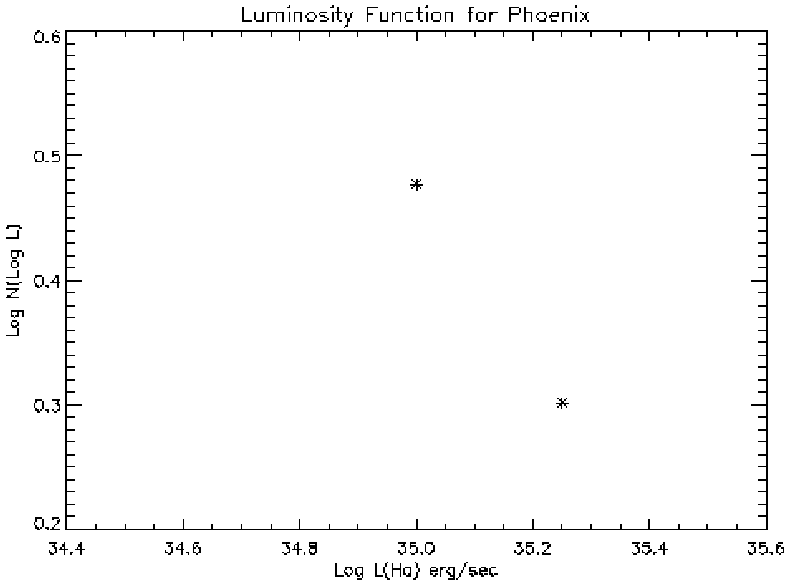

Figure 4.24: The First (and only) Luminosity Function for Phoenix Dwarf.

Chapter 5

Conclusions

5.1 Interpretation

Due to the capabilities of the wide-field MOSAIC images, significant numbers of H II regions within the dwarf irregular galaxies, NGC 6822, WLM, and Phoenix, where found. These new regions contribute significantly to the overall luminosity functions for the galaxies. While their characteristics are consistent with the previously determined properties of irregular galaxies (Kennicutt et al., 1998*a*), the contribution of these new regions present up to a 25% deviation in the total luminosity of the galaxys' H II regions.

Comparatively, the results for NGC 6822 nearly mimic the function derived by Hodge et al. (1988). The increase of the number of small and medium-sized regions, $10^{35} < L < 10^{36}$, highlight the possibility of significant star formation regions, missed by smaller, less deep surveys.

The luminosity function for WLM is different from the Hodge and Miller (1995) function. Because Hodge and Miller contribute some of their detection error to the atmospheric conditions, the deviation between the two functions can be considerably justified. Additionally, this paper included regions undetected or those deemed insignificant to the ultimate luminosity distribution.

While few points exist for the Phoenix luminosity function, the discovery of the H II regions is significant. Considered devoid of young stars until recently (Delgado et al., 1999), there is evidence of a burst of of star formation occurring less than 150 Myr ago. This, in conjunction with the new-found luminosity function delineates significantly more evidence for the existence of O and B stars.

Bibliography

[1] Delgado, Gallart, and Aparico. The stellar content of the local group dwarf galaxy phoenix. *AJ*, 118(862), 1986.

[2] Van den Bergh. The outer fringes of the local group. *AJ*, 107, 1994.

[3] Carroll et al. *An Introduction to Modern Astrophysics*. Addison Wesley, 1996.

[4] Hodge et al. The h ii regions of ngc 6822. i. an atlas of 157 h ii regions. *PASP*, 100(97), 1988.

[5] Hodge, Lee, and Kennicutt. The stellar content of the local group dwarf galaxy phoenix. *PSAP*, 101(32), 1989.

[6] Hodge and Miller. H ii regions in four galaxies in and near the local group. *ApJ*, 451(176), 1995.

[7] Paul Hodge. *The Stellar Content of the Local Group Dwarf Galaxy Phoenix*. University of Washington Press, 1981.

[8] Jacoby, Quigley, and Africano. Two-dimensional spectrophotometry of planetary nebulae by ccd imaging. *PASP*, 99(672), 1987.

[9] Kennicutt. Properties of h ii region populations in galaxies. i. the first-ranked h ii regions. *ApJ*, 334(114), 1988.

[10] Kennicutt and Skillman. H ii regions and abundances in the dark galaxy ddo 154 and the chemical evolution of dwarf irregular galaxies. *AJ*, 121(1461), 2001.

[11] Peimbert, Rayo, and Peimbert. Observations of faint h ii regions in our galaxy. *RMAA*, 1(289), 1975.

[12] Strobel, Hodge, and Kennicutt. H ii regions in seven dwarf irregular galaxies. *AJ*, 383(148), 1991.

[13] Thilker, Braun, and Walterbros. Hiiphot: Automated photometry of h ii regions applied to m51. *AJ*, 120(3070), 2000.

[14] Youngblood and Hunter. H ii luminosity functions and size distributions of h ii regions in irregular galaxies. *ApJ*, 519(55), 1999.